Seminar series nr 106

Investigating vegetation changes in the African Sahel 1982-2002: a comparative analysis using Landsat, MODIS and AVHRR remote sensing data

Martin Sjöström

2004
Geobiosphere Science Centre
Physical Geography and Ecosystems Analysis
Lund University
Sölvegatan 12
S-223 62 Lund
Sweden

Investigating vegetation changes in the African Sahel 1982-2002: a comparative analysis using Landsat, MODIS and AVHRR remote sensing data

---

Martin Sjöström, 2004

Degree-thesis in Physical Geography and Ecosystem Analysis
Supervisor
Lars Eklundh

Department of Physical Geography and Ecosystem Analysis
Lund University

Abstract

There has been much debate concerning the concept of degradation and desertification in semi-arid lands, in particular semi-arid Sub-Saharan Africa, during the last two decades. However, recent findings suggest a consistent trend of increasing satellite-derived vegetation greenness in much of the African Sahel as interpreted from Pathfinder Advanced Very High Resolution Radiometer (AVHRR) Normalized Difference Vegetation Index (NDVI) data for the period 1982-1999. The Sahel has suffered several devastating droughts and famines during recent decades and an increasing trend in NDVI could be interpreted as a vegetation recovery from the severe droughts of the 1980s, as preliminary analysis indicate an increase in rainfall during this period. This study includes an analysis of spatial and temporal trends of vegetation, covering the years 1982-2002, for areas in the western, eastern and central parts of the African Sahel in order to try to verify and explain the observed increasing trends in NDVI. By implementing two change detection techniques, visual interpretation and change vector analysis of high resolution satellite sensor data, it was observed that vegetation patterns differed, with recent year satellite imagery showing higher amounts of vegetation. It was, however, observed through comparison of phenological activity between the years of the acquired imagery that seasonal differences exist, most probably due to different climatic conditions preceding the recordings. Linear trend regressions of NOAA NDVI and rainfall data was analysed, and separately show increasing trends. The relationship between these two was also established by regression. The observed recent trends in vegetation activity cannot entirely be explained by increasing rainfall but rather as a combination of driving forces.

Sammanfattning

Det så kallade Sahelbältet, sträcker sig från Atlanten i väst till Röda Havet i öst och gränsar mellan Sahara i norr och de mer tropiska områdena i söder. Regionen är torr med oregelbunden nederbörd och anknyts ofta till begreppen ökenspridning och markförstörelse. I kontrast mot spekulationer kring dessa begrepp visar nyligen utförda studier på en signifikant positiv trend i Pathfinder Advanced Very High Resolution Radiometer (AVHRR) Normalized Difference Vegetation Index (NDVI) över stora delar av Sahel mellan åren 1982-1999. NDVI är ett satellitbaserat vegetationsindex som används för att få en uppfattning om vegetationens mängd och dess tillstånd. Den påvisade positiva trenden kan tolkas som en återhämtning av växtlighet efter de återkommande perioder av torka som drabbade Sahel under 70- och 80-talet. I syfte att verifiera och förklara den observerade ökningen i NDVI, ingår i denna studie analyser av både rumsliga och temporala trender mellan åren 1982-2002 för områden i östra, centrala och västra Sahel. Den rumsliga delen innefattas av visuell tolkning samt en radiometriskt baserad förändringsanalys kallad ”change vector analysis”. Dessa metoder tillämpades på högupplöst (30 x 30 m) satellitdata. Resultaten visar på en ökad växtlighet, då det förekommer mer vegetation i senare års satellitdata. Dock visade jämförelser av fenologisk aktivitet mellan de analyserade bildparen att säsongsskillnader existerade. Analys av tidsserier från Global Inventory and Mapping Studies (GIMMS) NDVI samt nederbörd visade på en positiv trend mellan åren 1982-2002. I flera studier har man funnit ett samband mellan NDVI och nederbörd, således tillämpades en regressionsanalys för att undersöka hur väl dessa två korrelerade med varandra. Resultaten pekar på att den observerade ökningen i NDVI inte helt och hållet kan förklaras med ökad nederbörd. Ökningen tros istället vara ett resultat av en kombination av faktorer.

Acknowledgements

I would like to give a special thanks to my supervisor PhD Lars Eklundh, at the Department of Physical Geography and Ecosystems Analysis at Lund University, for his guidance, valuable advice and feedback. I would also like to thank the following persons for providing materials and ideas.

Jonas Ardö	Department of Physical Geography, Lund University.
Bodil Elmqvist	Center for Environmental Studies, MICLU, Lund University.
Pontus Olofsson	Department of Physical Geography, Lund University.
Lennart Olsson	Center for Environmental Studies, MICLU, Lund University.
Micael Runnström	Department of Physical Geography, Lund University.
Jonas Åkerman	Department of Physical Geography, Lund University.

Table of contents

1 Introduction

1.1 Background

1.1.1 Sahel

Sahel is a large stretch of land running from the Atlantic Ocean in the west to the Red Sea in the east. It is a transition zone paralleling the equator, flanked by the arid Sahara to the north and the wetter more tropical areas to the south.

The climate of this region is mostly arid and it is hard to manage agriculture with little and erratic precipitation. The area is predominantly covered by sparse savannah vegetation of grasses and shrubs. In terms of annual precipitation, the Sahel receives on average between 100 mm and 600 mm of rainfall. The Sudanian zone to the south is occasionally included, where rainfall may exceed 800 mm (Seaquist, 2001).

There is no such thing as normal rainfall in the Sahel (Hulme, 2001). Rainfall is unreliable and the Sahel region is well known for its twin environmental problems of drought and desertification (Agnew & Chappell, 1999). The people of Sahel have suffered several yearlong periods of drought during the last century: in 1903-1905, 1911-1914, 1966-1974 and 1979-1987 respectively (Matsson & Rapp, 1991).

During recent decades, the world has witnessed reports on droughts in the Sahel, as in the 1970s when several climatologists noted a downward trend in rainfall. The crisis became an international aid effort in which the Food and Agricultural Organisation (FAO) of the United Nations (UN) announced that some areas run risk of imminent human famine and virtual extinction of herds vital to nomad populations (Agnew & Chappell, 1999). The same concerns continued through the 1980s as Copans (1983) estimated 100,000 drought related deaths in the Sahel. In 1984 the world's attention was drawn to the country of Sudan as the famine seriously affected approximately 10 per cent of the 22 million inhabitants (Olsson, 1993). Observations showed a downward trend in rainfall reporting that the drought in the Sahel had not yet ended (Hulme, 2001). It is clear from an observational record of the 20th century that the desiccation in Sahel has no equal, with the magnitude and duration being unprecedented (Middleton & Thomas, 1997).

1.1.2 Concept of desertification and degradation

The Sahel-Sudan zone is often described as undergoing environmental degradation. Active processes included might be deforestation, soil erosion, soil nutrient depletion etc. Desertification is a concept often used when all these processes are organized. But several authors (Helldén, 1991; Olsson, 1993; Nicholson et al., 1998) have noted that the empirical basis for the belief that desertification would be taking place at the scales and with the speed, that has been assumed, is weak (Rasmussen et al, 2001).

The concept and definition of desertification was adopted by the United Nations Conference on Environment and Development as:

Land degradation in arid, semi-arid and dry sub-humid areas resulting from various factors, including climatic variations and human activities (UN, 1992).

In order to fully understand the concept of desertification, one must also define land degradation. Many definitions are available and Williams & Balling (1995) define land degradation in dry lands as:

Reduction of biological productivity of dry land ecosystems, including rangeland pastures and rainfed and irrigated croplands, as a result of an acceleration of certain natural, physical, chemical and hydrological processes, including erosion and deposition by wind and water, salt accumulation in soils, groundwater and surface runoff, a reduction in the amount or diversity of natural vegetation, and a decline in the ability of soils to transmit and store water for plant growth.

Speculations about land clearance on rainfall, land degradation and the climatology of droughts have remained unresolved and the concept of desertification has persisted.

1.1.3 Greening of the Sahel

In contrast to the speculations of degradation and desertification, recent observations indicate that the Sahel belt may be undergoing some very rapid environmental changes as parts of this otherwise drought-stricken area appear to have greened up during the last 20 years.

With the Normalized Difference Vegetation Index (NDVI) providing important source of information on vegetation function as well as on land use and land cover, 10-day maximum value composites (MVCs) from the NASA/NOAA Pathfinder AVHRR Land (PAL) was used to create annual times series of NDVI for the Sahel region (Eklundh & Olsson, 2003).

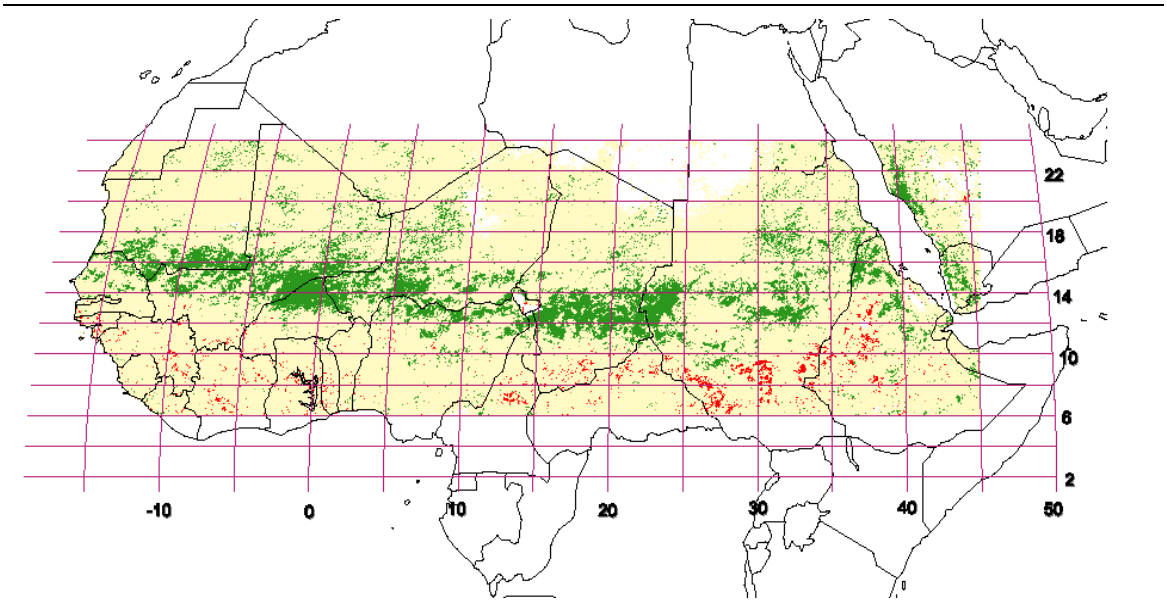

Figure 1.1. Linear trend of NDVI in Sahel over the period 1982-1999. Dark green = strong positive trend, yellow = no clear trend, red = negative trend. Source: Eklundh & Olsson, 2003

Results showed a strong increase in seasonal NDVI over large areas in the Sahel during the time period (Figure 1.1). Methods for estimating growing season parameters was

based on robust mathematical curve fitting, resulting in smooth approximations of the original noisy time-series (Eklundh & Olsson, 2003).

The observed trend could be interpreted as a recovery from the Sahelian drought years during the mid 1980s as several previous studies have shown a positive relationship between NDVI and rainfall (Prince, 1991; Nicholson & Farrar, 1994).

1.2 Objectives

This study aims at verifying and explaining the satellite-observed changes in the Sahelian region of Africa. A comparison of high-resolution (30 x 30 m) satellite data from the beginning of the 1980s and recent satellite images will be made in order to investigate what is inside the NOAA 8 x 8 km pixels.

Main objectives include; (i) investigate whether vegetation is related to NDVI change by examining differences or similarities between areas with significantly changed NDVI and areas with no significantly changed NDVI; (ii) investigate whether precipitation in the region is related to NDVI change over time by examining differences or similarities between areas with significantly changed NDVI and areas with no significantly changed NDVI and by comparing the NOAA satellite record with rainfall data.

1.3 Study Areas

The study areas of the Sudan, the Central African Republic, Niger and Mauritania are all in the semi-arid zone of Sub-Saharan Africa. The specific geographic locations of the four study areas are as follows: latitude 11° 34'N, and longitude 32° 8'E for the Sudan, latitude 7º 14'N and longitude 21º 55'E for the Central African Republic, latitude 14º 27' and longitude 6º 30 'E for Niger, and finally, latitude 15º 54'N and longitude 10º 11'W for Mauritania.

1.3.1 The Sudan

The first and eastern study area (Figure 1.2) lies within the Sudan states of Southern Kordofan, White Nile and Upper Nile, situated in the central part of the Sudan. Once considered as the "breadbasket of the Arab World" (Olsson, 1993; Ayoub, 1999), the Sudan has 7 per cent of the continents cropland, 13 per cent of its pasture and 10 per cent of its live stock population (Ayoub, 1999). The Blue and White Nile Rivers, tributaries to the great Nile River, which merge in the capital of Khartoum, generally contribute water for the agricultural irrigated practices on the country's vast arable tracts.

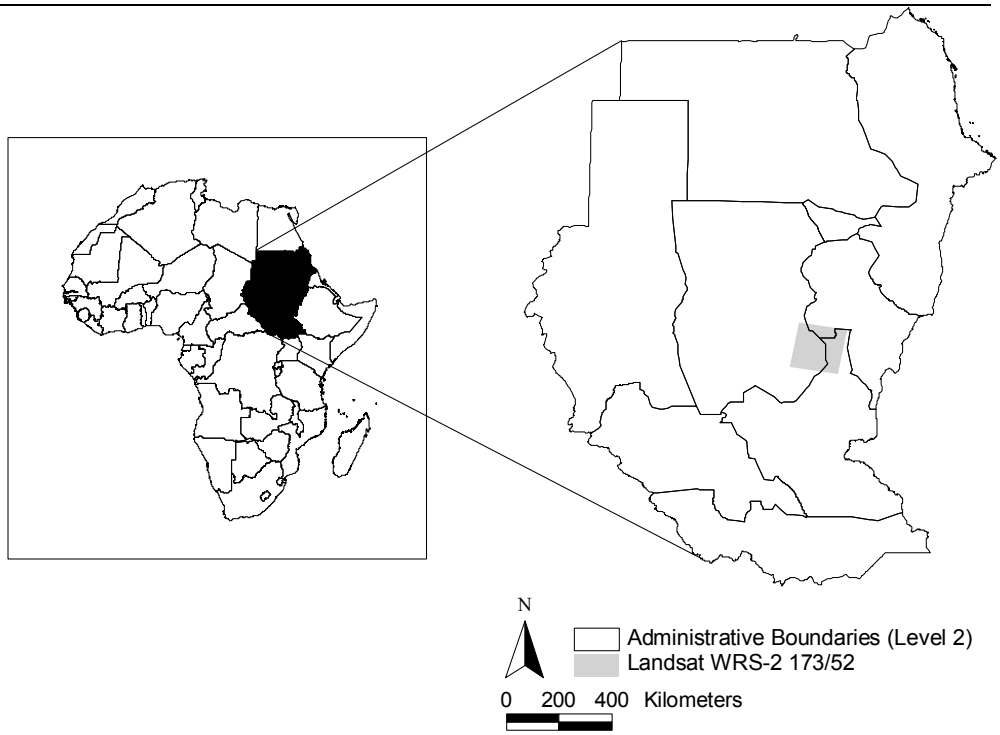

Figure 1.2. Africa, the Sudan, its administrative boundaries and the WRS-2 Landsat scene used in this study.

The nation of the Sudan has had its fair share of tragedies, ranging from armed conflicts (between religious fractions) to food crises. In the beginning of the 1980s Africa's largest nation was struck by severe famine, as rainfall was exceptionally low, causing substantial deficit in grain production. The famine affected half the population and in the hardest hit areas, death rates reached 3 per cent of the inhabitants per month. It is believed that the famine was primarily not caused by shortage of food, but rather by poor distribution of food (Olsson, 1993).

The climate in central Sudan is generally semi-arid with annual rainfall varying from 400 mm to 800 mm (Ayoub, 1999). As seen in Figure 1.3 temperature usually reaches its maximum during March and April, while the rainy-season usually extends from July to October.

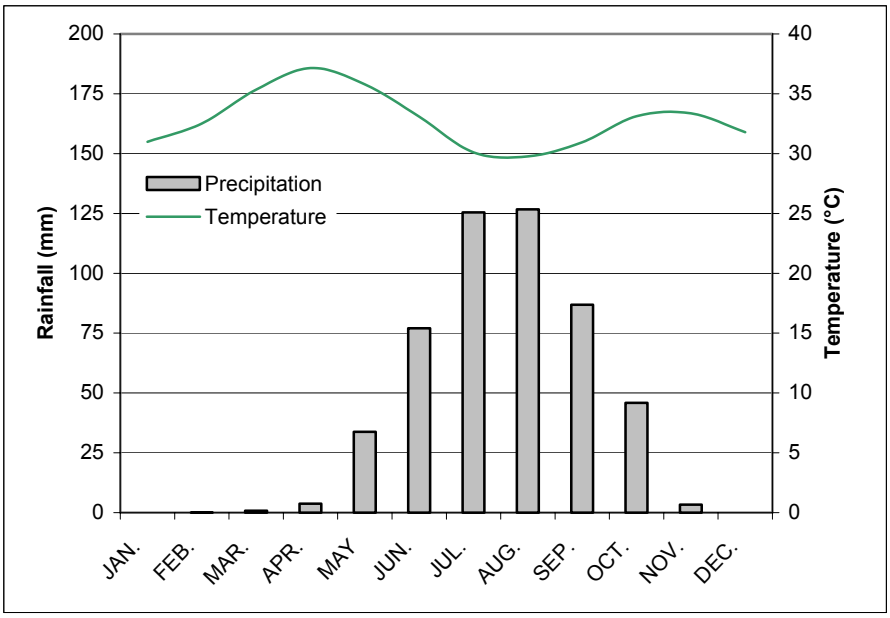

Figure 1.3. Monthly mean precipitation (mm) 1960-1999 and monthly mean of the daily 24-hour temperature (˚C) 1964-1999. Data collected from nearest ground station, Er-Renk (Sudan). Source: Global Historical Climatology Network (GHCN)

Vegetation in this part of central Sudan is mainly comprised of tall grasses and bushes and Acacia woodland mainly located in the vicinity of the White Nile River (Ayoub, 1999).

According to FAO (1997) this area is covered by Vertisols except alongside the White Nile where frequently flooded Entisols called Fluvents exist due to water deposited sediments. Vertisols are clay soils characterized by usually forming deep wide cracks from the surface and downwards when they dry out, thus becoming extremely solid. This together with the fact that Vertisols become sticky during wet seasons make them difficult to harness for agricultural purposes if not correctly managed. Vertisols stand apart from other soils as they have a vertic horizon containing high amounts of clay minerals or products of weathered rock that have the characteristics of clay (FAO-UNESCO, 1997; USDA-NRCS 1999; Batjes, 2001).

Entisols are soils of recent origin characterized by little horizontization as their parent material has only just accumulated. These soils have a wide geographic distribution and can be found in any climate under any vegetation but are often found on floodplains, delta deposits or steep slopes (FAO-UNESCO, 1997; USDA-NRCS, 1999; Batjes, 2001).

1.3.2 Central African Republic

The second study area (Figure 1.4) lies within the state of Haute-Kotto situated in the central part of the Central African Republic (C.A.R). Once, a former French territory, the C.A.R. has a population of approximately 3.5 million and forms a part of the landlocked West African Region. As the country holds vast amounts of natural wooded areas, forestry is a key element of the economy together with agriculture. The C.A.R. has also been embarking in diverse industrial ventures such as mining and oil industries. However these activities do not significantly contribute to the countries Gross Domestic Product (GDP).

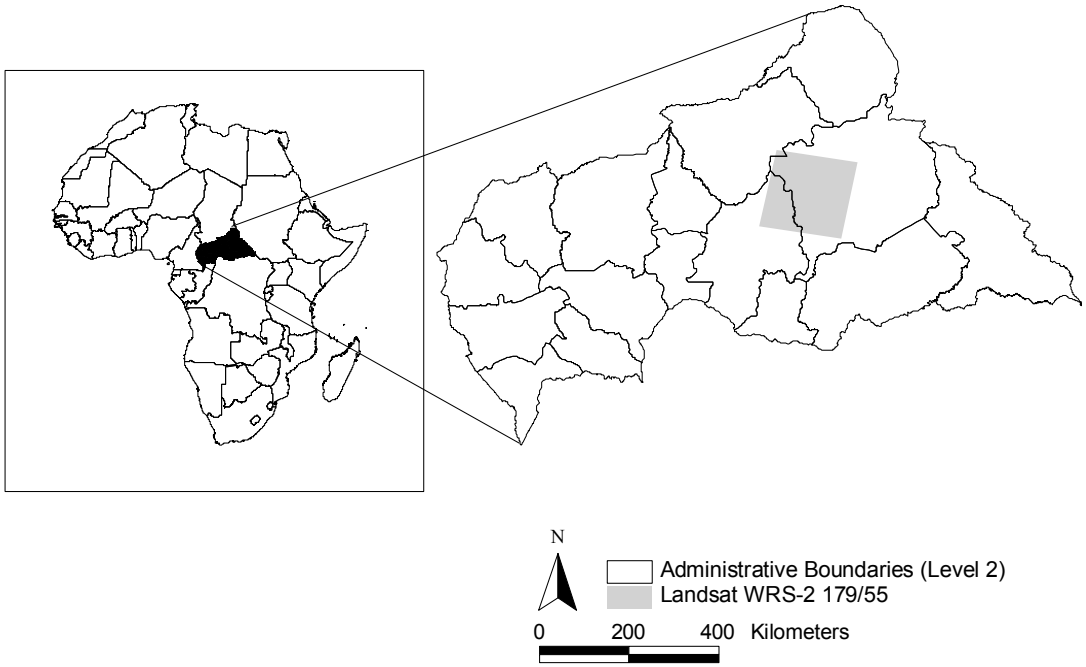

Figure 1.4. Africa, the Central African Republic, its administrative boundaries and the WRS2 Landsat scene used in this study.

The C.A.R. is one of the wettest nations in the Sahel and did not suffer as seriously as the more arid countries in this region from the droughts of the 1970s and 1980s. The East and West Gulf of Guinea countries underwent less irregular rainfall (even though below normal) than the rest of Sahel during these periods (Gommes & Petrassi, 1996). In the northern and central parts of the C.A.R., the climate is drier and more irregular than that compared to the southern parts with rainfall varying between 1200 mm to 1500 mm annually. Temperature usually reaches its maximum around March and April.

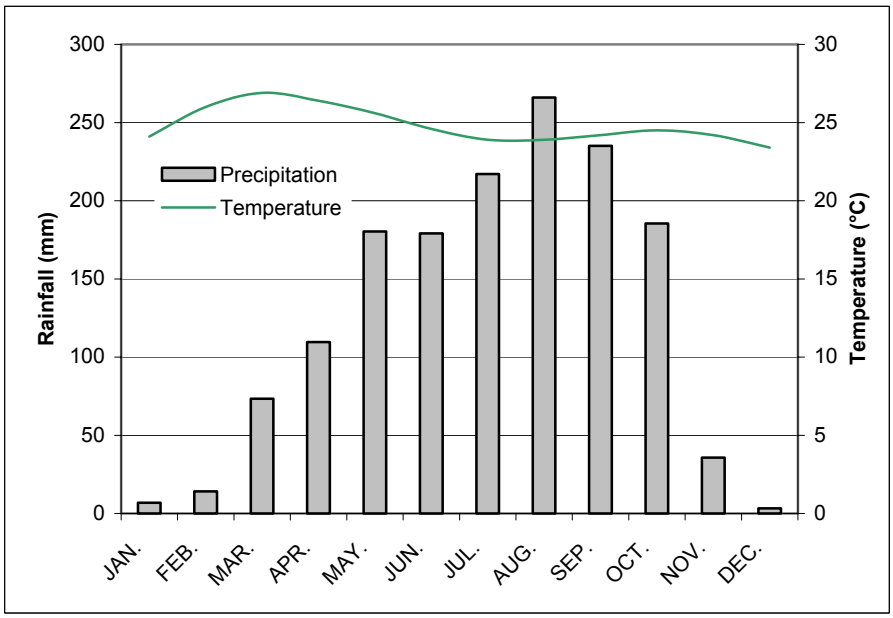

Figure 1.5. Monthly mean precipitation (mm) 1941-1989 and monthly mean of daily temperature (˚C). 1951-1989. Data collected from nearest ground station, Bria (Central African Republic). Source: GHCN

The study area lies within a transition zone between the spiny herbaceous vegetation of the extreme north and the dense rain forest of the south. The characteristic vegetation is thus mainly savannah derived from light forest interspersed with gallery forest (Mayaux et al. 1999).

According to FAO (1997), the soil resources in this area can be divided into two regions. Stretching from the north to southeast is a broad belt of Entisols and to the centre and southwest are the Oxisols.

Oxisols are characterized by containing high amounts of oxides called "sesquioxides", formed as a result of chemical weathering and the presence of warm temperatures combined with heavy rainfall. A combination of heavy rainfall and rapid uptake by vegetation quickly removes nutrients from the soil thus making it chemically poor and not well suited for agriculture (FAO-UNESCO, 1997; USDA-NRCS, 1999; Batjes, 2001).

1.3.3 Niger

The third study area (Figure 1.6) is located in the southern parts of the country of Niger within the districts of Maradi and Tahoua. Being the largest state in West Africa, Niger has a population of approximately 11 million. The nations economy primarily centres on subsistence agriculture, animal husbandry and re-export trade. Like most Sahelian land-locked countries Niger is dependant on agricultural exports, and economic growth is held back by poor transport links with the rest of the world (Ford, 2004).

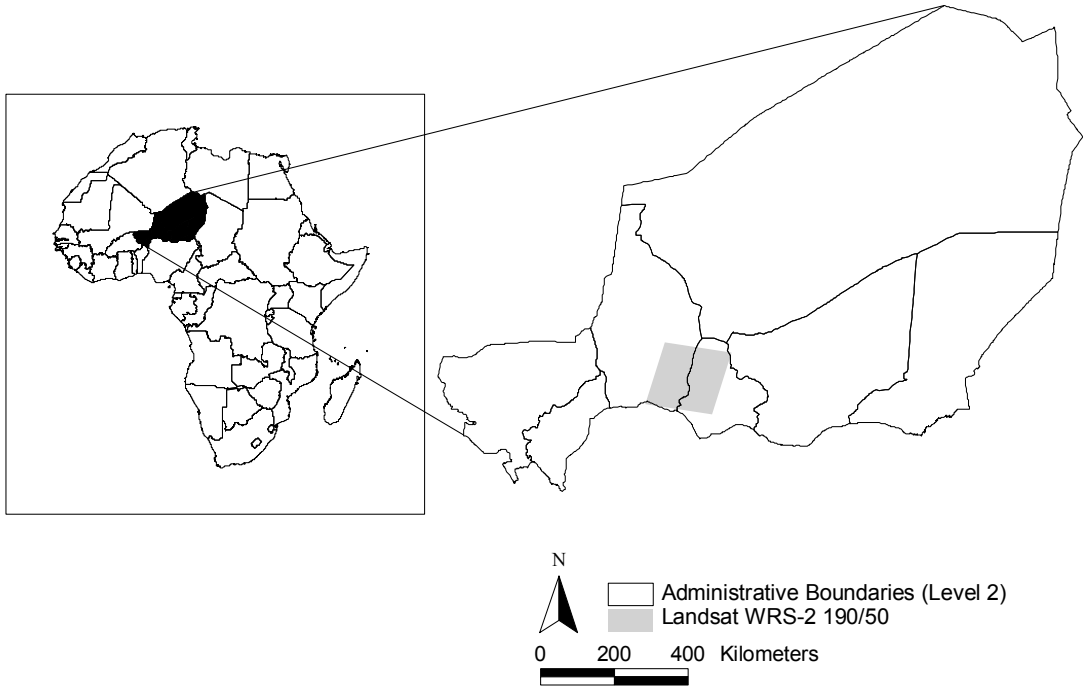

Figure 1.6. Africa, Niger, its administrative boundaries and the WRS-2 Landsat scene used in this study.

With rainfall being as erratic and variable as Sudan, Niger was hit hard by the droughts in the 1970s and 1980s. Characterized by high temporal rainfall variability, precipitation

falls during 3 to 4 months (usually June to September) with an annual total precipitation of approximately 300-600 mm. Temperature usually reaches its maximum around April-May (Wezel & Haigis, 2002).

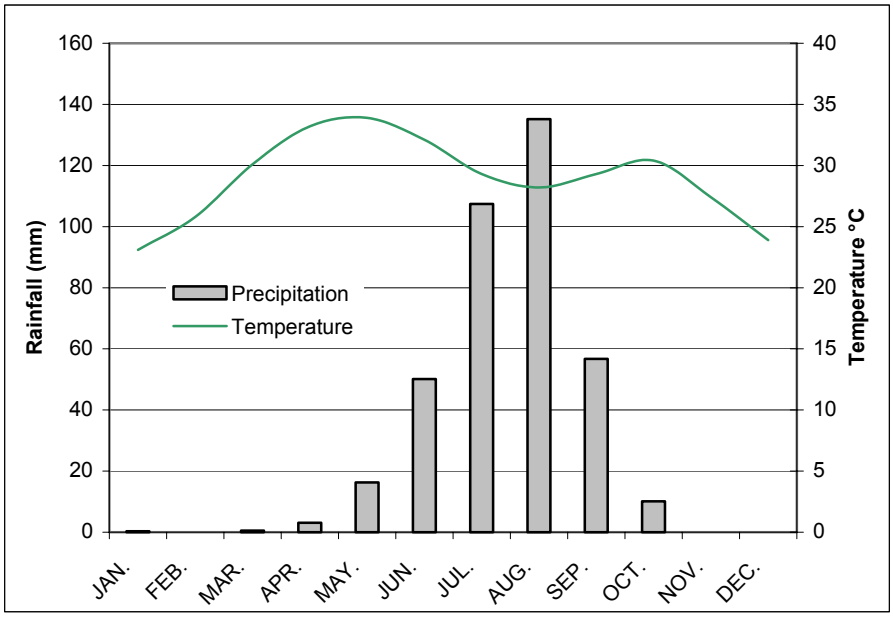

Figure 1.7 Monthly mean precipitation (mm) 1921-1989 and monthly mean of daily temperature (˚C) 1951-1990. Data collected from nearest ground station, Tahoua (Niger). Source: GHCN

Grass and shrub savannas are characteristic for southern Niger and its amount is, as in most parts of the Sahel, heavily dependent on precipitation. Vegetation usually has a short life cycle with trees generally located within and around water holding depressions (Wezel & Schlecht, 2004).

Soils in this area mainly consist of Alfisols and Inceptisols along waterways running through the area. Alfisols are generally fertile soils, productive for agriculture, as they have a favourable moisture balance. They are usually found in flat or gently sloping regions where climate is warm with distinct dry and wet seasons (FAO-UNESCO, 1997; USDA-NRCS, 1999; Batjes, 2001).

Inceptisols are young soils just starting to show horizon development. These soils are commonly found in any type of environment structured in alluvium floodplains and delta deposits. By and large these soils make excellent soils for agricultural production (FAO-UNESCO, 1997; USDA-NRCS, 1999; Batjes, 2001).

1.3.4 Mauritania

This western study site (Figure 1.8) is located in the southern parts of the country of Mauritania within the district of Hodh El Gharbi in close proximity to the Mali border. Approximately 2.5 million people live in Mauritania, which is situated within the vast western part of the Saharan desert. A large amount of Mauritania's land is covered with sand making its agricultural resources limited.

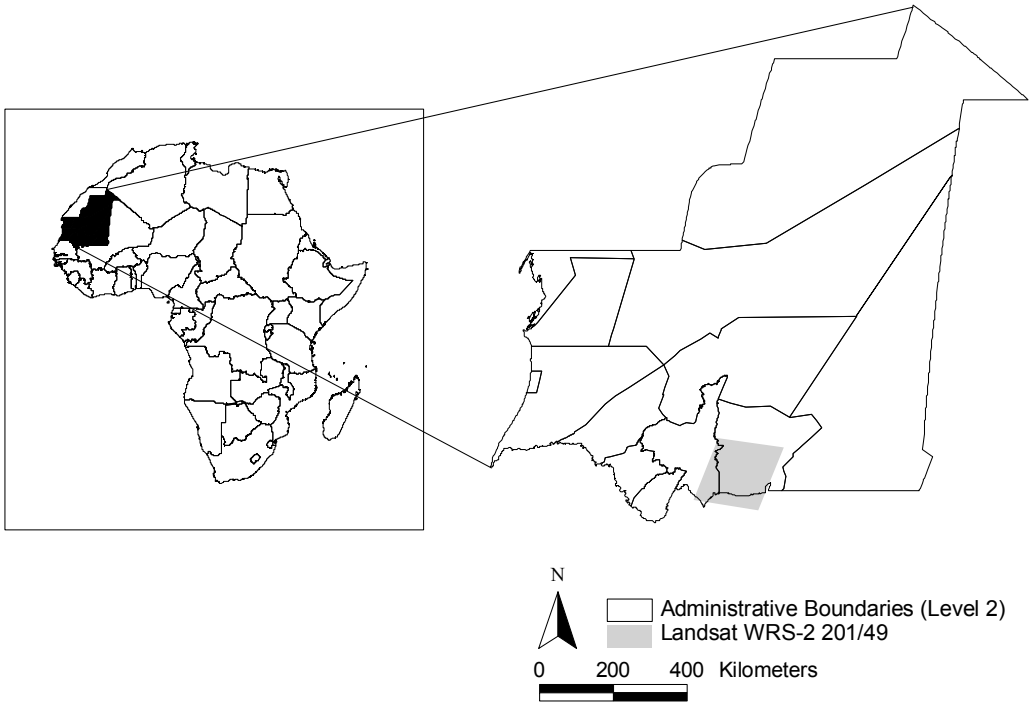

Figure 1.8. Africa, Mauritania, its administrative boundaries and the WRS-2 Landsat scene used in this study.

Mauritania's agro-climatic conditions are not favourable for cultivation and as less than one per cent of the country's land is arable Mauritania's economy heavily depends on its export of mineral deposits and fish. Agricultural practices are profoundly conditioned by an erratic climate and rarely meet 50 per cent of the country's food requirements (Josserand & Silva, 2002).

Mauritania has experienced frequent droughts since the 1960s and was hit hard by the 1984 drought, severely affecting the country's resources for food. This downward trend in rainfall was followed by a series of about-average years during the 1990s. Compared to other countries such as neighbouring Senegal the situation in southern Mauritania was somewhat worse due to its position in the immediate southern fringe of the Sahara Desert where rainfall is spatially and temporally erratic (Thiam, 2003).

Runs of dry seasons and wet seasons are a typical feature of the southern parts of Mauritania as climate is generally hot and dry with annual rainfall varying between 250-400 mm. The wet season usually begins in July and extends to October and a long dry season with minimum temperatures around 15 ˚C in January and maximum temperature regularly exceeding 40 ˚C in April–May (Van Asten et al. 2004).

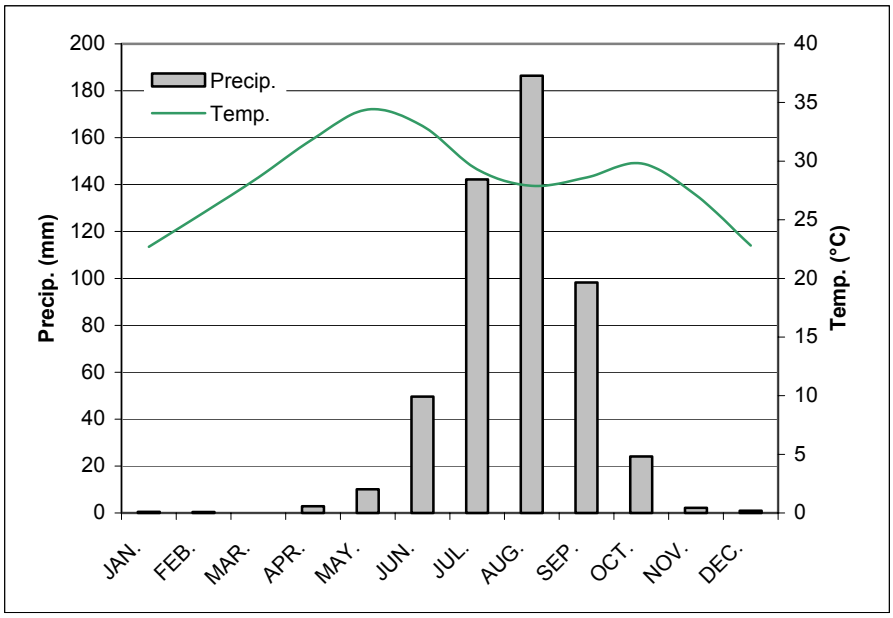

Figure 1.9. Mean monthly precipitation (mm) 1950-1999 and mean monthly temperature (˚C) 1951-1990. Data collected for nearest station, Nioro Du Sahel (Mali). Source: GHCN

In contrast to the northern parts of Mauritania where plant life is not abundant, vegetation in the southern parts principally consists of grasses and bushes. Trees are rare and are mostly restricted to beds of wadis in or beneath which water continues to flow.

Soils in this area mainly consist of fine sandy Entisols to the north and Alfisols and Inceptisols to the south (FAO-UNESCO, 1997).

2 Theoretical background

2.1 Satellite sensors used in this study

2.1.1 Advanced Very High Resolution Radiometer

The use of the Advanced Very High Resolution Radiometer (AVHRR) provided by the National Oceanic and Atmospheric Administration (NOAA) polar satellite series present the opportunity to study land surface variables at a regional and global scale. Although recent satellite sensors may provide improved global land satellite data the AVHRR record, which extends from July 1981 through 2003/2004, is an invaluable source of historical land information (Diouf & Lambin, 2001).

Spectral vegetation indexes, such as the NDVI, designed to enhance the contributions of vegetation properties, are the most used land products derived from the AVHRR sensors. AVHRR reflectance data is recorded at a maximum resolution of 1 km and the NDVI product is generally produced at an even further reduced resolution, usually 8 km, in favor of providing global or large-scale coverage. The AVHRR-NDVI provides for the longest record for monitoring global vegetation dynamics.

2.1.2 Thematic Mapper

Landsat 4, carrying the first Thematic Mapper (TM) sensor was launched in 1982. The TM sensor is an upgrade of the Multispectral Scanner Subsystem (MSS) on which efforts were made to incorporate improvements into a new instrument. The TM instrument is therefore based on the same technical principal as the MSS, but with a more complex design as it provides finer spatial resolution (30 m for bands 1-5, 7 and 120 m for band 6), improved geometric reliability, greater radiometric detail and more detail spectral information. The MSS only has four broadly defined spectral regions whereas the TM has seven, customized to record radiation of interest to specific scientific investigations (Campbell, 1996).

2.1.3 Enhanced Thematic Mapper Plus

The Enhanced Thematic Mapper Plus (ETM+) sensor carried by Landsat 7, launched in 1999, is an offshoot of the TM. The ETM+ sensor offers several enhancements over the Landsat 4 and 5 TM sensor, including increased spectral information content, improved geodetic accuracy, reduced noise, reliable calibration, the addition of a panchromatic band, and improved spatial resolution of the thermal band (60 m compared to the TMs 120 m). The same resolution as the TM bands 1-5 and 7 apply for the ETM+ (Masek et al, 2001).

2.1.4 Moderate Resolution Imaging Spectroradiometer

The Moderate Resolution Imaging Spectroradiometer (MODIS) instrument was first launched on the Terra Satellite in late 1999 and has been designed to provide improved monitoring for land, ocean and atmosphere research. It combines characteristics from the AVHRR and TM with added spectral bands in the middle and long-wave infrared. Data is provided at spatial resolutions of 250 m, 500 m, and 1 km. For improved atmospherics and cloud characterization spectral channels have been included to allow for the removal

of atmospheric effects on surface surveillance and atmospheric measurements (Justice et al., 1998).

The MODIS science team has developed a series of algorithms in order to provide data products to meet the needs of global change research, giving scientist the opportunity to utilize such basic surface variables as spectral reflectance, albedo and land surface temperature as well as higher order variables, such as vegetation indices (NDVI, EVI), leaf area index (LAI), fraction of absorbed photosynthetically active radiation (FPAR), active fires, burned area and snow and ice cover (Justice et al., 1998).

2.2 Normalized Difference Vegetation Index

Red light is absorbed by photosynthetic pigments found in green leaves while near-infrared light either passes through or is reflected by leaf tissues regardless of colour. Areas of bare soil will thus appear similar in both the red and near infrared (NIR) wavelengths while areas under vegetation will appear bright in the NIR and dark in the red part of the spectrum. By using these wavelengths, vegetation indices can be produced. One of these is the NDVI, which is the most widely used vegetation index.

NDVI is the ratio of the NIR and red radiances and is calculated from atmospherically corrected reflectances from the red and NIR channels as:

$$NDVI = \frac{NIR - RED}{NIR + RED}$$

This ratio yields a measure of the photosynthetic capacity and produces values in the range of -1.0 to 1.0, where vegetated areas will have values greater than zero and negative values indicate non-vegetated surface features such as water, snow or clouds.

2.2.1 NOAA AVHRR NDVI

NOAA AVHRR data is used to generate NDVI images of large portions of the Earth on a regular basis in order to provide a global set of images that show seasonal and annual changes over vegetative cover. The AVHRR NDVI is created using data from channel 1 and channel 2 in the following way:

$$AVHRR\ NDVI = \frac{Channel\ 2 - Channel\ 1}{Channel\ 2 + Channel\ 1}$$

Channel 1 is in a part of the spectrum where chlorophyll causes considerable absorption of incoming radiation, and Channel 2 is in a spectral region where spongy mesophyll leaf structure leads to considerable reflectance.

2.2.2 Landsat NDVI

The TM and ETM+ bands 3 and 4 provides red and NIR measurements and can therefore be used to generate NDVI data sets using the following formula:

$$Landsat\ NDVI = \frac{Band\ 4 - Band\ 3}{Band\ 4 + Band\ 3}$$

Two of the key differences between AVHRR and Landsat derived NDVI products is the resolution and the difference in spectral range in the red and NIR channels. As the AVHRR sensor has a wider spectral range in both the red and NIR channels, the probability of atmospheric effects interfering with the surface signal increases as compared to the TM and ETM+ sensors. The AVHRR, also, has a resolution that is much lower than the TM and ETM+ sensors. The Landsat TM and ETM+ consequently offer far greater detail, though it is able to provide less aerial extent. Thus, the AVHRR data is more appropriate for creating frequent global NDVI products while the Landsat TM/ETM+ data is most useful for creating images with greater detail covering smaller areas.

2.3 Change detection

Change detection is the process of identifying the state of an object by observing it at different times. In general, change detection involves the application of multi-temporal datasets to quantitatively analyse the temporal effects of an object.

Lu et al. (2004) state that the following conditions must be satisfied in order to implement a change detection analysis: (i) precise registration of multi-temporal images; (ii) precise radiometric and atmospheric calibration or normalization between multi-temporal images; (iii) similar phenological states between multi-temporal images; and (iv) selection of the same spatial and spectral resolution images if possible.

2.4 Tasseled Cap

The concept of tasseled cap transformation is a useful tool for compressing spectral data into a few bands associated with physical scene characteristics. It is a linear transformation of data that projects soil and vegetation information into a single plane in multispectral data space. Three different types of tasseled cap transformations have essentially been developed based on the TM, the first one on digital number (DN) (Crist & Cicone, 1984), the second based on reflectance factor (Crist, 1985) and the third one based on at-satellite reflectance (Huang et al. 2002).

While the similar spectral characteristics of TM and ETM+ may imply direct applicability of DN and reflectance factor transformations to ETM+ images, an at-satellite reflectance based tasseled cap transformation for Landsat 7 has been developed. Huang et al. (2002) presents a number of causes for the need of such a transformation; (i) the reflectance-based transformation is based on ground measurements with little

atmospheric effects. Applying this transformation accordingly indicates that satellite images require atmospheric correction. Although several algorithms for atmospheric correction have been developed, many users are still concerned with possible unknown errors that may arise due to lack of data; (ii) use of the digital number (DN) based transformation in multiscene applications can be problematic as changing sun illumination geometry strongly affects DN, and thus affecting the derived tasseled cap value.

2.5 Change vector analysis

When land undergoes change or disturbance during a certain amount of time, its spectral appearance normally changes. Change vector analysis (CVA) has been variously applied and advanced since its application by Malila (1980) to characterize change magnitude and direction in spectral space from a first to a second date. The total change magnitude and nature of change per pixel is computed by determining the Euclidian distance and the angle between end points through *n*-dimensional change space. In this study a 2-dimensional change space was represented by the calculations of indices through tasseled cap transformation.

A number of potential advantages of CVA over other methods for change detection are presented by Johnson & Kasischke (1998). These include: (i) capability to concurrently process and analyse change in all multispectral input data layers; (ii) the capability to detect both changes in land cover and condition; and (iii) computation and separation of multidimensional change images that retain this information and facilitate change interpretation and labelling.

3 Materials and methods

3.1 Remote sensing data

3.1.1 Landsat data

Factors greatly controlling the selection of Landsat images included; (i) the time-integrated values and amplitude values within NOAA AVHRR-derived images; (ii) landscape characteristics, no complex surfaces such as rugged or mountainous landscapes which would require topographic correction; (iii) accessibility of cloud free image data; and last but not least (iv) availability of free Landsat data.

A set of 4 pairs of Landsat 5 (TM) and Landsat 7 (ETM+) geometrically corrected scenes (Table 3.1) were acquired from the Global Land Cover Facility (GLCF) and have undergone systematic radiometric and geometric correction using standard methods.

Table 3.1. Eastern, central and western Sahel Landsat 5 and 7 satellite images obtained from the GLCF geocover database[1].

WRS P/R	Landsat 5 Acq. Date	Landsat 7 Acq. Date	Location
173/52	1984-11-18	1999-11-04	Sudan
179/55	1984-11-28	1999-11-30	C.A.R
190/50	1986-09-28	2001-09-29	Niger
201/49	1984-10-21	1999-10-07	Mali, Mauritania

During processing of Landsat raw data, data undergoes two-dimensional resampling according to user-specified parameters including output map projection, rotation angle, pixel size, and resampling kernel. The WGS-84 ellipsoid was employed as the earth model for coordinate transformation. The end result is thus a geometrically rectified product with minimum distortions related to the sensor and earth. The positional accuracy is 50 m root mean square (RMS) (EarthSat, 2004).

3.1.2 AVHRR data

15-day composite NDVI data, from the AVHRR flown on the NOAA-series satellites, were acquired from the Global Inventory Mapping and Monitoring System (GIMMS) for the Sahel area from 1981 to 2002. This 8 by 8 km dataset supplies essential information on annual vegetation amplitudes and length of seasonal cycles and was used to assess and study trends and phenology between the dates of the 1984 and 1999 Landsat scenes.

3.1.3 MODIS data

MODIS NDVI and EVI (Enhanced Vegetation Index) with a spatial resolution of 250 m were acquired for each Landsat WRS-2 path/row from the earth Observing Systems (EOS) Data Gateway, and served as supplementary data to assist in the interpretation process. The products have been validated, meaning that product uncertainties are well defined over a number of representative conditions.

[1] http://glcf.umiacs.umd.edu

3.2 Rainfall data

Mean monthly precipitation data covering the years 1982-1999/2000 from climate stations in Er-Renk (the Sudan), Bria (C.A.R.), Maradi (Niger) and Nioro Du Sahel (Mali) was acquired from the Global Historical Climatology Network (GHCN). This is a comprehensive global climate data set frequently used to monitor and detect climate change (GHCN, 2004).

3.3 Pre-processing procedures

3.3.1 Pre-processing of Landsat data

In order to take advantage of the superior radiometric calibration of ETM+, Landsat 5 DNs can be converted to Landsat 7 DNs by using the following equation:

$$DN7_{\lambda} = DN5_{\lambda} \cdot slope + intercept$$

Where:

λ	= TM band number
$DN7$	= Converted Landsat 5 DNs
$DN5$	= Original Landsat 5 DNs

Band #	Slope	Intercept
1	0.9398	4.2934
2	1.7731	4.7289
3	1.5348	3.9796
4	1.4239	7.032
5	0.9828	7.0185
7	1.3017	7.6568

Table 3.2. Slope and intercept values for converting Landsat 5 DNs to Landsat 7 DNs.

These values are based on relationships upon comparison between Landsat 5 and 7 near-simultaneous data acquisitions using radiometric regression equations. Results showed that band-to-band relationships between the two data sets appeared very high with r^2 ranging from 0.9912 (Band 1) to 0.9996 (Band 4) (Vogelmann et al. 2001).

By using the following set of gain and bias values, the derived image is then treated as an ETM+ DN image in calculating at-satellite reflectance and tasseled cap transformation:

Band #	Gain	Bias
1	0.7756863	-6.1999969
2	0.7956862	-6.3999939
3	0.6192157	-5.0000000
4	0.6372549	-5.1000061
5	0.1257255	-0.9999981
7	0.0437255	-0.3500004

Table 3.3. Radiance gain and bias values used after conversion of Landsat 5 DNs to Landsat 7 DNs.

The purpose with a radiometric correction is to convert the DN-values to absolute radiance values. Absolute radiance is required when utilizing temporal data that may come from different sensors (normalize) or when using radiation as input to mathematical/physical models. Radiance is given by the following equation:

$$L_\lambda = GAIN_\lambda \cdot DN_\lambda + BIAS_\lambda$$

Which is also expressed as:

$$L\lambda = \frac{LMAX_\lambda - LMIN_\lambda}{QCALMAX - QCALMIN} \cdot QCAL - QCALMIN + LMIN$$

Where:

λ	= ETM+/TM band number
L	= Spectral radiance at the sensors aperture in watts
$GAIN$	= Rescaled gain (contained in the product header)
$BIAS$	= Rescaled bias (contained in the product header)
$QCAL$	= The quantized calibrated pixel value in DN
$LMIN$	= The spectral radiance that is scaled to QCALMIN
$LMAX$	= The spectral radiance that is quantized to QCALMAX
$QCALMIN$	= The minimum quantized calibrated pixel value
$QCALMAX$	= The maximum quantized calibrated pixel value

For relatively clear Landsat scenes, a reduction in between scene variability can be achieved through normalization for solar irradiance by converting spectral radiance to effective at-satellite reflectance, or in-band planetary albedo (Markham & Barker, 1986). This is given by:

$$\rho_\lambda = \frac{\pi \cdot L_\lambda \cdot d^2}{ESUN_\lambda \cdot \sin(\theta)}$$

Where:

λ	= ETM+/TM band number
ρ	= Unit less planetary reflectance
L	= Spectral radiance at the sensors aperture in watts
d	= Earth-Sun distance in astronomical units
$ESUN_\lambda$	= Mean solar exoatmospheric irradiances (Table 3.4)
θ	= Solar zenith angle in degrees

Table 3.4. ETM+ and TM solar spectral irradiances, bands 1-5 and 7.

Band #	Mean solar exoatmospheric irradiance (w/m^{2}μm)
1	1969.00
2	1840.00
3	1551.00
4	1044.00
5	225.70
7	82.07

3.3.2 Pre-processing of AVHRR data

Data from GIMMS have been corrected for sensor degradation with a technique based on stable desert targets. It also includes corrections for stratospheric volcanic aerosols from volcanic eruptions in 1982 and 1991 (Slayback et al., 2003). Maximum NDVI was used as a compositing technique with cloud screening based on AVHRR channel 5 thermal threshold values. No correction has been applied to correct for atmospheric effects due to water vapor, Rayleigh scattering or stratospheric ozone. Artifacts in NDVI due to satellite drift have been corrected by using an empirical mode decomposition technique (EMD). NDVI data are archived as 8-bit (unsigned) integer values and to recover the true NDVI range the following expression was used before mapping the data to Albers equal-area projection:

$$NDVI = (DN - 1) \cdot 1000 / 249 - 50$$

3.3.3 Pre-processing of MODIS data

This data has been geometrically and radiometrically corrected and are supplied as HDF-EOS grid files (Hierarchical Data Format), which contain multidimensional arrays of data elements. In order to save space, a specified HDF-EOS object first had to be extracted in binary format from the grid files and then converted to 8-bit (unsigned) integer before mapping it to a sinusoidal projection.

3.4 Visual analysis

3.4.1 Method

The land cover and land use interpretation was done through visual analysis of Landsat TM and ETM+ false colour composite satellite imagery by the use of available ancillary data. Land cover delineation was primarily based on ancillary and spectral data content while land use information primarily was segmented from aspects as pattern, shape and size. The first step of the visual analysis process was to create a preliminary legend of possible land cover classes for the area in order to define land cover classes from major land cover types. Delineation of major land cover types was based on the following ancillary data:

- Africover Project (Africover, 2004) This dataset is based on observable characteristics verified in the field. Cover classes are defined with the Land Cover Classification System (LCCS). Land cover and land use data has been produced from visual interpretation of digitally enhanced LANDSAT TM images (Bands 4, 3 and 2) acquired mainly in the between the years 1994-1999.

- Vegetation map of Central Africa derived from satellite imagery. This is a vegetation map at a 1:5.000.000 scale with a detailed description of vegetation classes and their distributions. This map is based on coarse resolution satellite imagery (NOAA AVHRR 5 km dataset) (Mayaux et al., 1999).

- Data from the U.S. Geological Survey's (USGS) Africa Land Cover Characteristics Data Base (USGS, 2004). These data are based on 1 km NOAA AVHRR data spanning from April 1992 to March 1993.

- MODIS-vegetation indices acquired from the Earth Observing System (EOS) Data Gateway. Spanning throughout the year 2000 in order to get an overall grasp of the density and temporal pattern of vegetation cover.

Table 3.5. Description of primary land cover and land use types used in this study.

Class Name	Description
1. Cultivated 1a. Irrigated 1b. Rainfed	Fields where crops and fallow land is dominant. Thus, a presence of a clear cultivation pattern with field boundaries. Divided into either irrigated or rainfed cropland depending on closeness to water.
2. Naturally Vegetated 2a. Grassland 2b. Open shrubland and herbaceous vegetation 2c. Closed shrubland 2d. Open trees and herbaceous vegetation 2e. Closed woodland	Areas where trees, shrubs and herbaceous vegetation are present. Primarily based on ancillary data and MODIS-NDVI.
3. Primarily non vegetated 3a. Barren or sparsely vegetated	Barren or sparsely vegetated areas with low or no vegetation cover. These are areas with low productivity primarily barren areas or areas with sparse herbaceous or woody vegetation.
4. Water	Areas enclosed by water. Inland water bodies.

The visual analysis and delineation was done by structuring a GIS environment that would allow displaying multiple band combinations and ancillary data in a set of linked windows. Land cover was then segmented in zones with different dominant land uses based on the interpretation of the landscape patterns, beginning with the most highly contrasting features first.

3.4.2 Cover classes

The land cover classes refer to the dominant class in the delineated polygon. Combinations of classes are given in a single polygon where areas were estimated to have an open cover. As seen in Table 3.6, *closed cover* is more than approximately 70 % of the classified perimeter, consequently a dense cover of vegetation. Open or very open cover, simply called *open***,** are areas with between approximately 70 % and 20 % of the classified perimeter, thus a moderately dense cover of vegetation. *Sparsely covered* areas occupy approximately less than 20 % of the ground, thus areas with low density vegetation cover.

Table 3.6.Description of land cover types used in this study.

Land cover types	**Description**
Barren or sparsely vegetated	Land primarily barren or areas with sparse vegetation covering approximately < 20 % of the delineated polygon.
Grassland	Land covered with approximately > 20 % herbaceous vegetation and with woody vegetation covering approximately < 20 % of the delineated polygon.
Open shrubs and herbaceous vegetation	Mixed class. Land with herbaceous vegetation and a woody cover covering approximately > 20% and < 70 % of the delineated polygon.
Closed shrubland	Land with a dense cover of shrubs covering approximately > 70% of the delineated polygon.
Open trees and herbaceous vegetation	Mixed class. Land with herbaceous vegetation and a woody cover covering approximately > 20 % and < 70 % of the delineated polygon.
Closed woodland	Land with a dense cover of trees covering approximately > 70% of the delineated polygon.

3.5 Change vector analysis

Since visual analysis has a tendency to be based on subjective image interpretation a spectral change detection method of CVA was implemented as a complement.

The first step of the CVA method was to apply a tasseled cap transformation based on at-satellite reflectance as described by Huang et al. (2002). This generates components of greenness and brightness and defines the new coordinate system on which the CVA is based. Thus, as a pixel undergoes change during a certain time-interval, its position in the defined coordinate system will change. (Kauth & Thomas, 1976)

Table 3.7. gives the coefficients for the derived tasseled cap transformation based on at-satellite reflectance. Values are weights where some are negative and others positive. For example, the highest coefficients for greenness are those of the red (negatively loaded)

and NIR (positively loaded) wave bands. This highlights the red-infrared contrast to better discriminate between vegetated areas. Thus, this index is similar to that of an NDVI image as they both reveal spatial pattern of green vegetation. Correspondingly, brightness values display and express the total reflection capacity of a surface cover, with small areas dominated by dispersed vegetation cover appearing brighter.

Table 3.7. Coefficients for deriving brightness and greenness tasseled cap images.

Index	Band 1	Band 2	Band 3	Band 4	Band 5	Band 7	Detection capabilities
Brightness	0.3561	0.3972	0.3904	0.6966	0.2286	0.1596	Soil characteristics
Greenness	-0.3344	-0.3544	-0.4556	0.6966	-0.0242	-0.2630	Green canopy characteristics State of vegetation cover

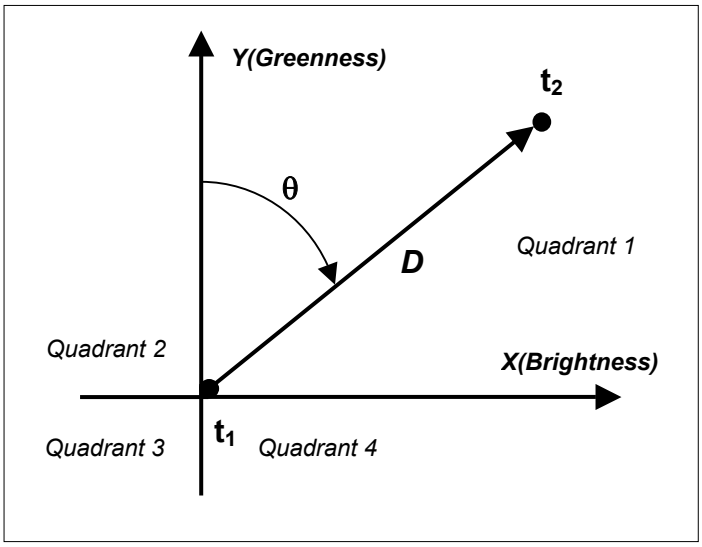

Figure 3.1. Representation of a change vector in a 2 dimensional Euclidian space with t_1 and t_2 being date one and two. Y and X correspond to at-satellite reflectance based tasseled cap indices greenness and brightness.

The second step was to calculate the direction of change based on the generated tasseled cap indices. The angle of the vector indicates the type of change that has occurred. This varies according to the number of components utilized. As only two have been used there can only be four focal types of changes per pixel. Angles of change are thus generated by the use of the following equations:

For quadrants 1 and 4:

$$\theta = 90° - \left(\arctan \frac{(y_{2-} y_1)}{(x_{2-} x_1)} \right)$$

For quadrants 2 and 3:

$$\theta = 270° - \left(\arctan \frac{(y_2 - y_1)}{(x_2 - x_1)} \right)$$

In order to produce a final image, representing angles in decimal degrees, clockwise from north, tasseled cap transform images first had to be divided in their separate change sector. Angles were then calculated relative to x- and y-axes using the two equations

above and then combined to generate a final image of angle change which represents the brightness difference and greenness difference from year one to year two, with each pixel in the final image designated an angle between 0° - 360°.

The third step was to calculate the magnitude among the spectral change vector. This was computed by simply calculating the Euclidian distance in a Pythagorean formula between two endpoints as:

$$D = \sqrt{(x_2 - x_1)^2 + (y_2 - y_1)^2}$$

3.6 Image comparability

In order to locate the TM and ETM+ images in the vegetation cycle a method of image comparability was used. NDVI was calculated for the TM and ETM+ datasets, and pixel values equal to the 8 x 8 km NOAA pixel were extracted and averaged for NOAA-TM-ETM+ comparability (Runnström, 2000).

4 Results

Five subsets were chosen for analysis, all approximately 16, 24 or 32 km x 16 km in size to be able to fit fully within homogenous regions of positive or no trend areas of the NOAA NDVI amplitude and integrated values imagery generated for every 8 x 8 km grid cell for the Sahel. These trends were based on smoothed annual values for 18 years (1982-1999) where seasonal amplitude is the difference between the seasonal peak of the smoothed NDVI and a base level and seasonal integral represent the area under the smoothed curve and the base level (Jönsson & Eklundh, 2002; Eklundh & Olsson, 2003).

Three sites were selected with a significantly strong positive trend in integrated NOAA NDVI and two with no significant trend in integrated NOAA NDVI. Two areas (Niger study sites 4A and 4B) were later added and were only subject to a general trend analysis, NDVI-rainfall regression and CVA.

Table 4.1. Derived subsets and study sites.

Site	Coordinates	Approximate size	NOAA trend, integrated/amplitude according to Eklundh & Olsson (2003)	Country
1A	31º42'00E, 12º00'00N	384km^2	Strong positive/Strong positive	Sudan
1B	32º39'00E, 10º44'00N	256km^2	Strong positive/Strong positive	Sudan
1C	31º55'00E, 10º54'00N	384km^2	No significant/Strong positive	Sudan
2A	21º55'00E, 6º40'00N	512km^2	No significant/No significant	Central African Republic
3A	10º42'00W, 16º43'00N	384km^2	Strong positive/Strong positive	Mauritania
4A	6º42'00E, 14º10'00N	1536km^2	Strong positive/Strong positive	Niger
4B	6º22'00E, 13º43'00N	192km^2	No significant/No significant	Niger

4.1 NDVI trends 1982 – 2002

Figure 4.1 - 4.3 show NDVI time series from GIMMS and linear trend for areas with, according to Eklundh & Olsson (2003), a strong positive trend in NOAA NDVI, whereas Figure 4.4 show time series from GIMMS and linear trend for an area with no significant trend. The slope of the linear trend through the time series was determined using least squares estimation.

A south-north difference is apparent when looking at the figures, as the droughts in the beginning of the 1980s seem to have struck harder on vegetation in the northern study sites 1A (Figure 4.1), 3A (Figure 4.2) and 4A (Figure 4.3) compared to study site 2A (Figure 4.4). Trends for all sites are positive, with five out of seven being statistically significant. Upon visual analysis, it is clear that the C.A.R. study site 2A time series does not show similar seasonal variation as the others. It is also clear that the annual maximum NDVI values for study sites 1A, 3A and 4A have increased throughout the time series, thus, an apparent increase in the vegetation index during the growing season.

Figure 4.1 shows the NDVI time series for study site 1A located in the Sudan. According to the linear trend, NDVI has increased 0.06 units over the 21 years. The difference in seasonal NDVI between the two studied years is apparent.

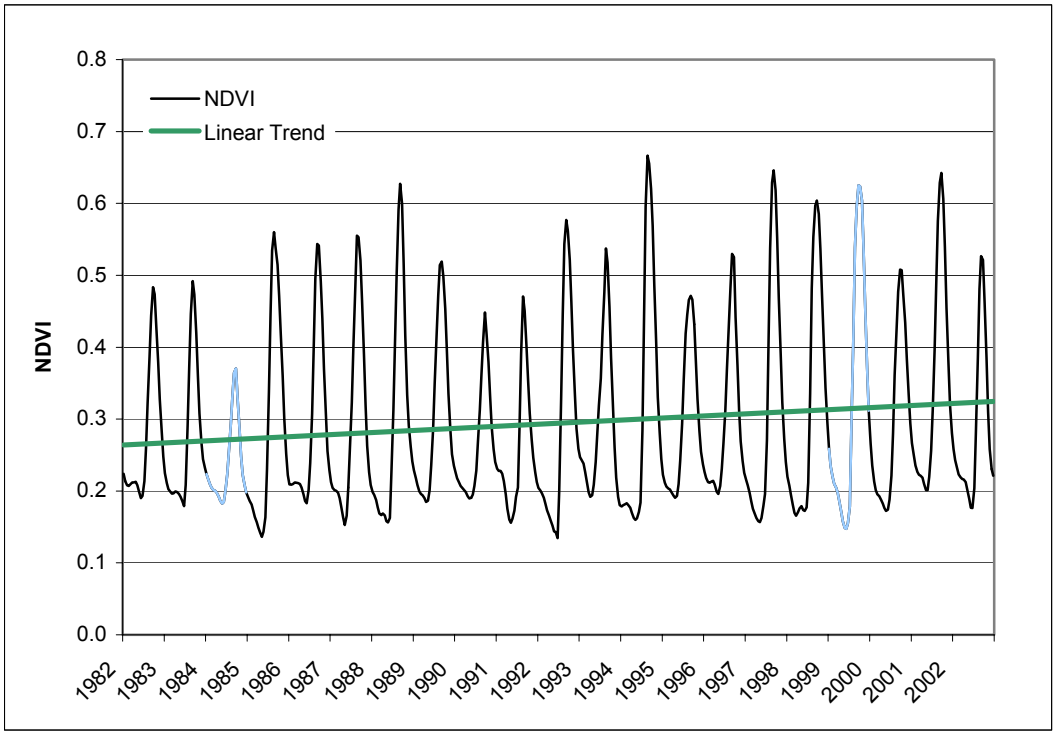

Figure 4.1. NDVI times series from 1982 - 2002 over study site 1A located in the district of Southern Kordofan in the country of Sudan. The site is approximately 384km^2 in size. Blue = Years of visual analysis and CVA (1984 and 1999). Data have been smoothed for visual presentation.

Figure 4.2 shows an NDVI time series for study site 3A, located in southern Mauritania. According to the linear trend, NDVI has increased by approximately 0.03 units over the 21 years. This area has low mean area NDVI values due to the sites large amount of primarily non-vegetated land.

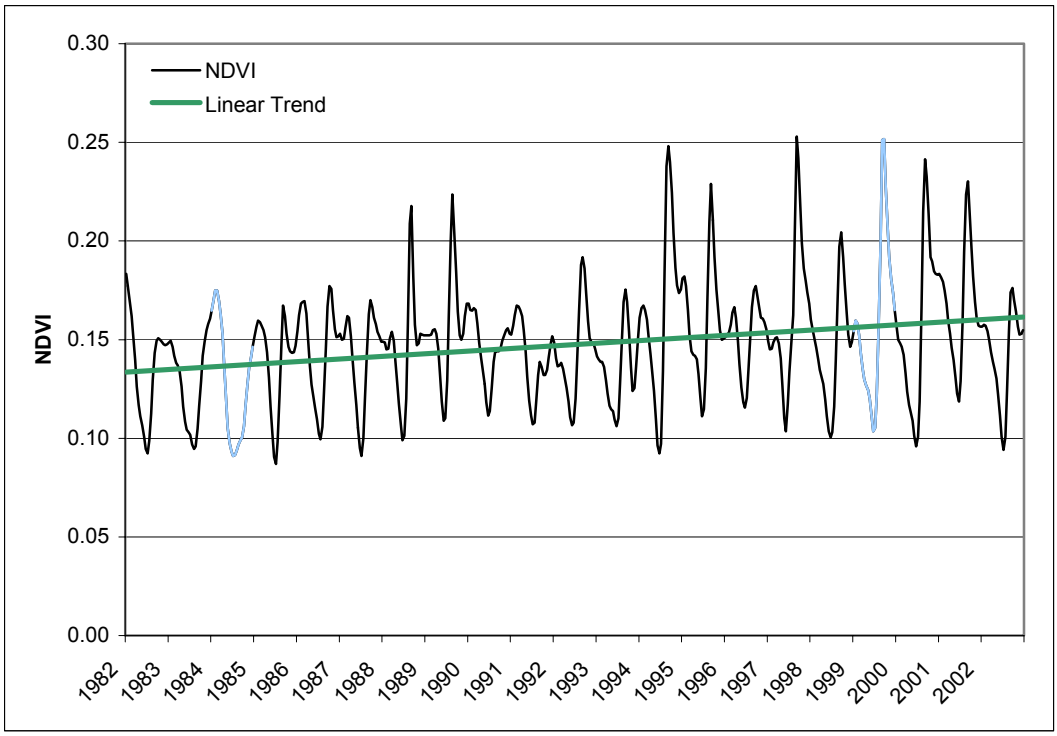

Figure 4.2. NDVI times series from 1982 - 2002 over study site 3A located in the district of Hodh el Gharbi in the country of Mauritania. Blue = Years of visual analysis and CVA (1984 and 1999). Data have been smoothed for visual presentation.

Figure 4.3 shows the NDVI time series for study site 4A located in southern Niger. For this area, NDVI has increased by approximately 0.04 units throughout the time series.

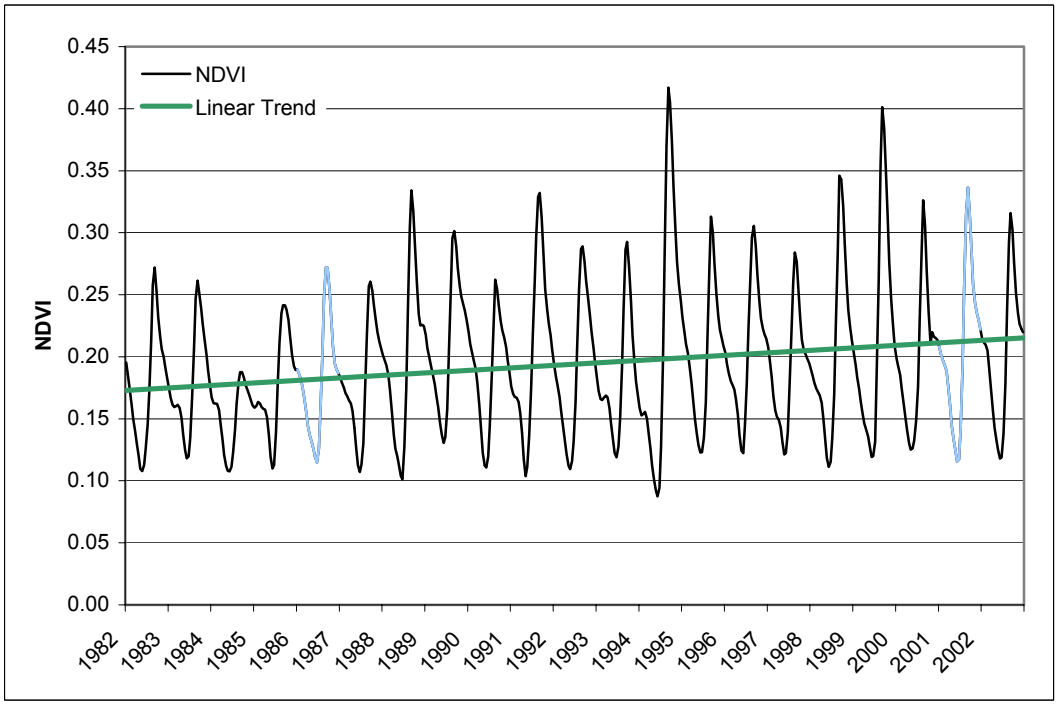

Figure 4.3. NDVI times series from 1982 - 2002 over study site 4A located in the district of Tahoua in the country of Niger. The site is approximately 1536km^2 in size. Blue=Years of visual analysis and CVA (1984 and 2001). Data have been smoothed for visual presentation.

Figure 4.4 shows the NDVI time series for study site 2A located in the C.A.R, a no significant trend area according to Eklundh & Olsson (2003). For this area, NDVI has increased by approximately 0.01 units throughout the 21-year period and maintains approximately similar seasonal NDVI values throughout the times series compared to Figures 4.1 – 4.3.

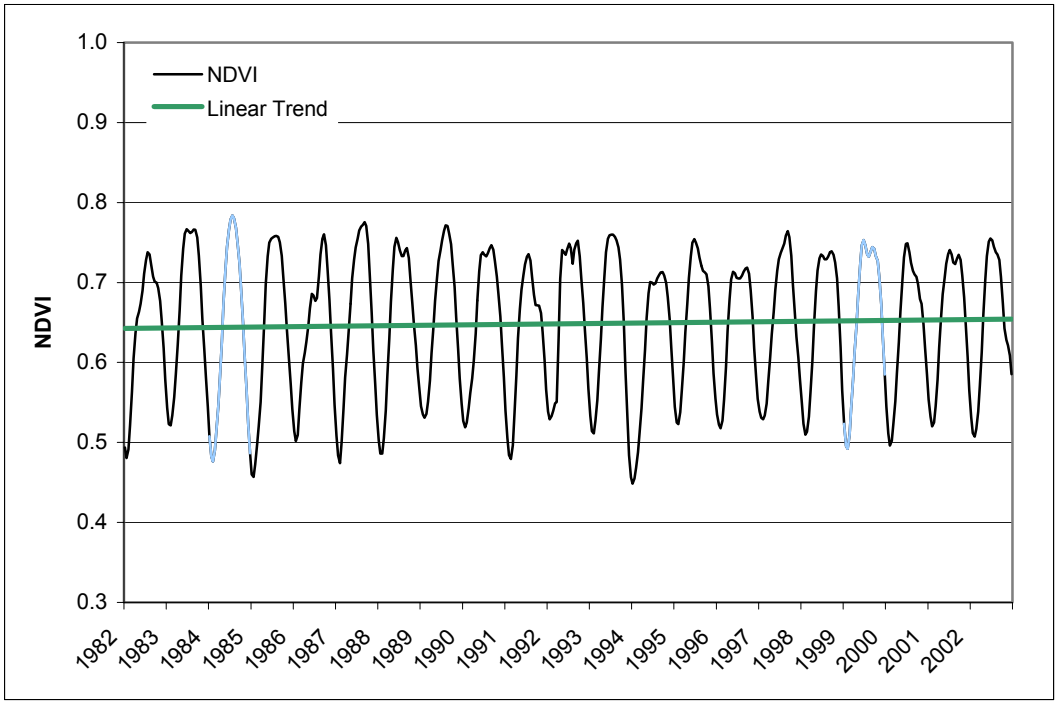

Figure 4.4. NDVI times series from 1982 - 2002 over study site 2A located in the district of Haute Kotto in the country of Central African Republic. Blue = Years of visual analysis and CVA (1984 and 1999). Data have been smoothed for visual presentation.

Table 4.2 shows a summary of the investigated NDVI trends for all studied sites. None of the studied sites indicated a negative slope coefficient with the highest and lowest unit increase in NDVI found for study site 1A and 2A respectively.

Table 4.2. Linear trend equation and unit increase in NDVI for studied sites, 1982 – 2002.

Site	NOAA trend, integrated/amplitude according to Eklundh & Olsson (2003)	Linear trend equation	Unit increase in NDVI, 1982-2002
1A	Strong positive/Strong positive	Y = 0.263572 + 1.21E-04	0.061*
1B	Strong positive/Strong positive	Y = 0.343198 + 9.73E-05	0.049
1C	No significant/Strong positive	Y = 0.338810 + 1.06E-04	0.053*
2A	No significant/No significant	Y = 0.642405 + 2.39E-05	0.012
3A	Strong positive/Strong positive	Y = 0.133780 + 5.44E-05	0.027*
4A	Strong positive/Strong positive	Y = 0.172942 + 8.35E-05	0.042*
4B	No significant/No significant	Y = 0.188779 + 6.05E-05	0.030*

** Statistically significant.*

4.2 Rainfall trends 1982 – 1999/2000

Figure 4.5, 4.6 and 4.7 shows mean monthly rainfall and linear trend for the Sudan, Mauritania and Niger study sites. The slope of the linear trend through the times series was calculated using the least square method.

None of the studied areas indicated a negative slope coefficient. The highest increase, between the years of 1982-1999/2000 was found for the Sudan sites were rainfall had increased by approximately 27 mm. For the studied site in Mauritania, rainfall had increased by 12 mm and for the studied areas in Niger, rainfall had increased by approximately 17 mm.

Collection of robust monthly and daily precipitation data for the study sites was a problematic task. It was especially difficult for the C.A.R. were the majority of rainfall datasets included a great deal of missing data values during late 1980s through the 1990s, and this site could thus not be included.

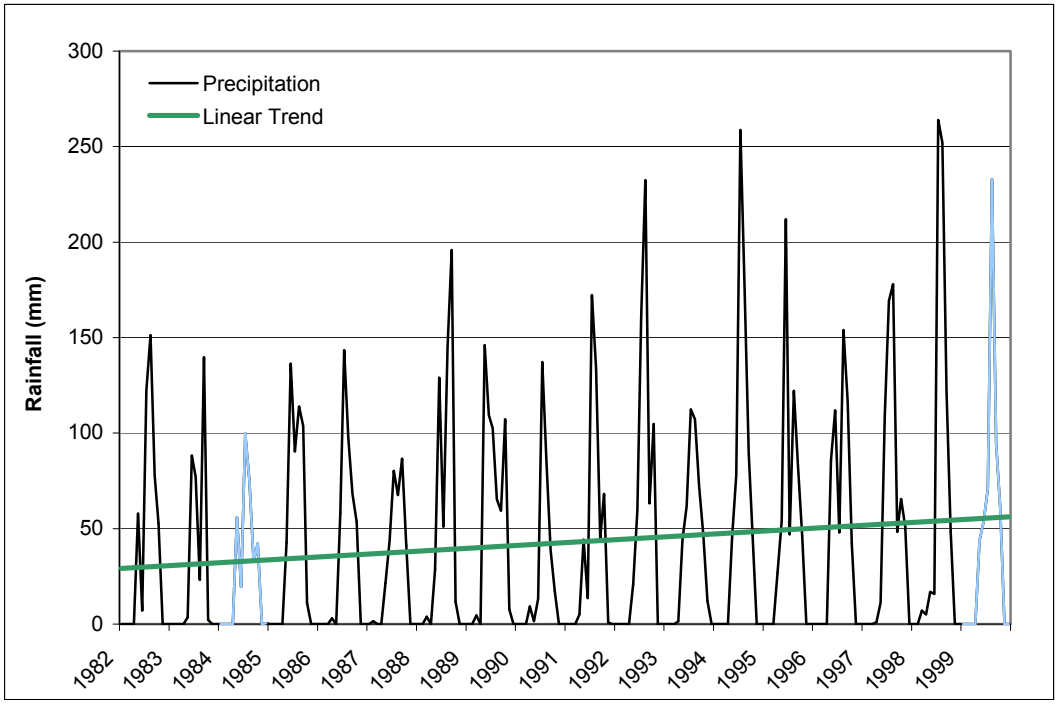

Figure 4.5. Mean monthly rainfall (mm) and linear trend between the years 1982-1999 for the Sudan study sites. Blue = Years of visual analysis and CVA (1984 and 1999). Data collected from closest ground station Er-Renk. Data have been smoothed for visual presentation.

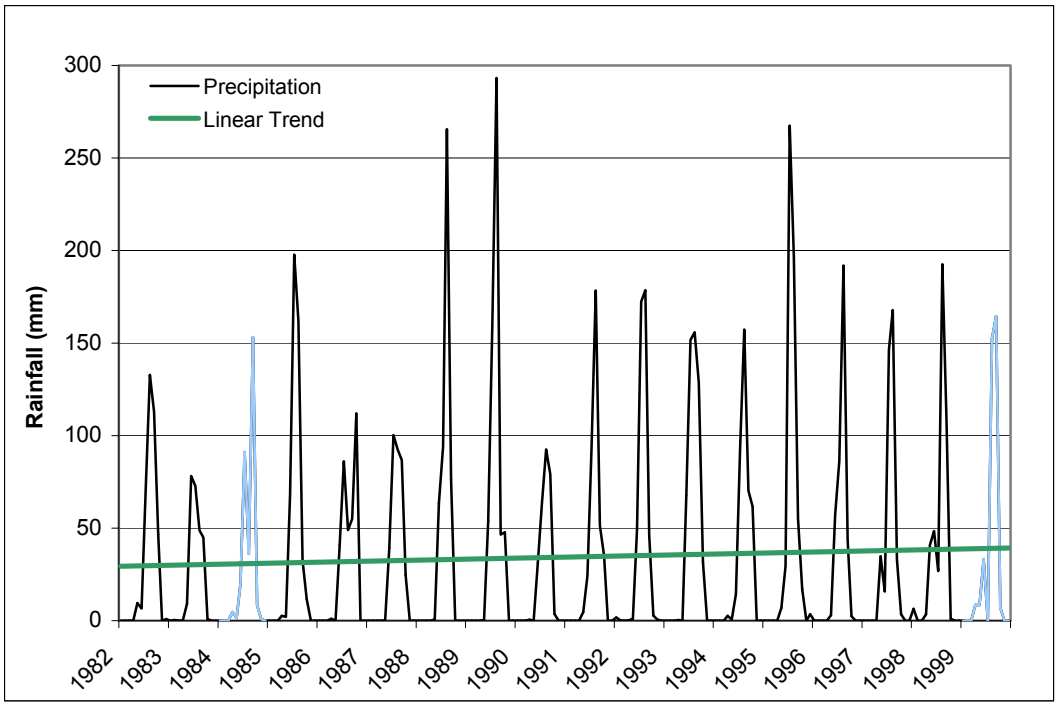

Figure 4.6. Mean monthly rainfall (mm) and linear trend between the years 1982-1999 for the Mauritania study site. Blue = Years of visual analysis and CVA (1984 and 1999). Data collected from closest ground station Nioro Du Sahel. Data have been smoothed for visual presentation.

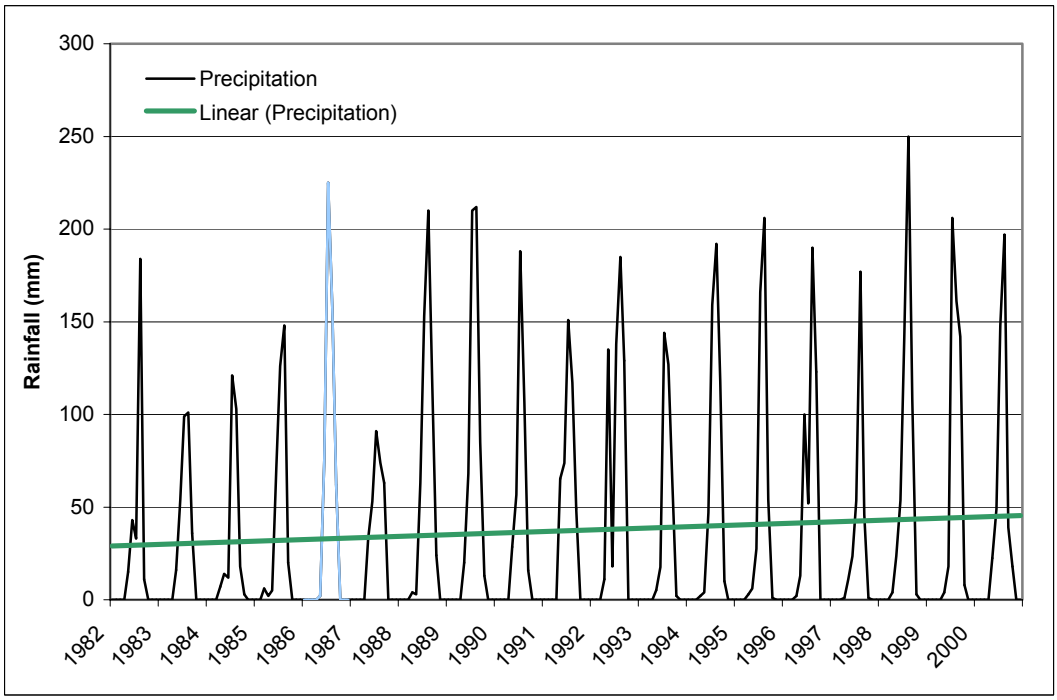

Figure 4.7. Mean monthly rainfall (mm) and linear trend between the years 1982-2000 for the Niger study sites. Blue = Years of visual analysis and CVA (1984. No available rainfall data for the year 2001.) Data collected from closest ground station Maradi. Data have been smoothed for visual presentation.

4.3 NDVI-rainfall regression

Previous studies have demonstrated, at the scale of the entire Sahelian region, that there is a strong relationship between rainfall and NDVI (Prince, 1991; Nicholson & Farrar, 1994). Annual rainfall and annual NDVI were analysed in order to eliminate time lag. Table 4.3 shows the results of the NDVI-rainfall regressions for all study sites except 2A, for which rainfall data was unavailable throughout most of the time period.

Site	NOAA trend, integrated/amplitude according to Eklundh & Olsson (2003)	R-squared value	P-value
1A	Strong positive/Strong positive	0.55	<0.001*
1B	Strong positive/Strong positive	0.27	0.028*
1C	No significant/Strong positive	0.44	0.005*
3A	Strong positive/Strong positive	0.19	0.065
4A	Strong positive/Strong positive	0.46	0.001*
4B	No significant/No significant	0.28	0.011*

** Statistically significant.*

Table 4.3. R-squared and P-values derived from the NDVI-rainfall regression for studied sites.

For five of the six areas, the relationship between NDVI and rainfall is significant but not strong. Of the two sites located in the Sudan, study site 1A (Figure 4.8) showed the best relationship with $R^2 = 0.55$ and a P-value of less than 0.001 while study site 1B showed a relationship with $R^2 = 0.27$ with $P = 0.028$ and study site 1C a relationship with $R^2 = 0.44$ with $P = 0.005$. Study site 4A located in Niger showed a relationship with $R^2 = 0.46$ and with $P = 0.001$ while site 4B showed a weaker relationship with $R^2 = 0.28$ and with $P = 0.011$.

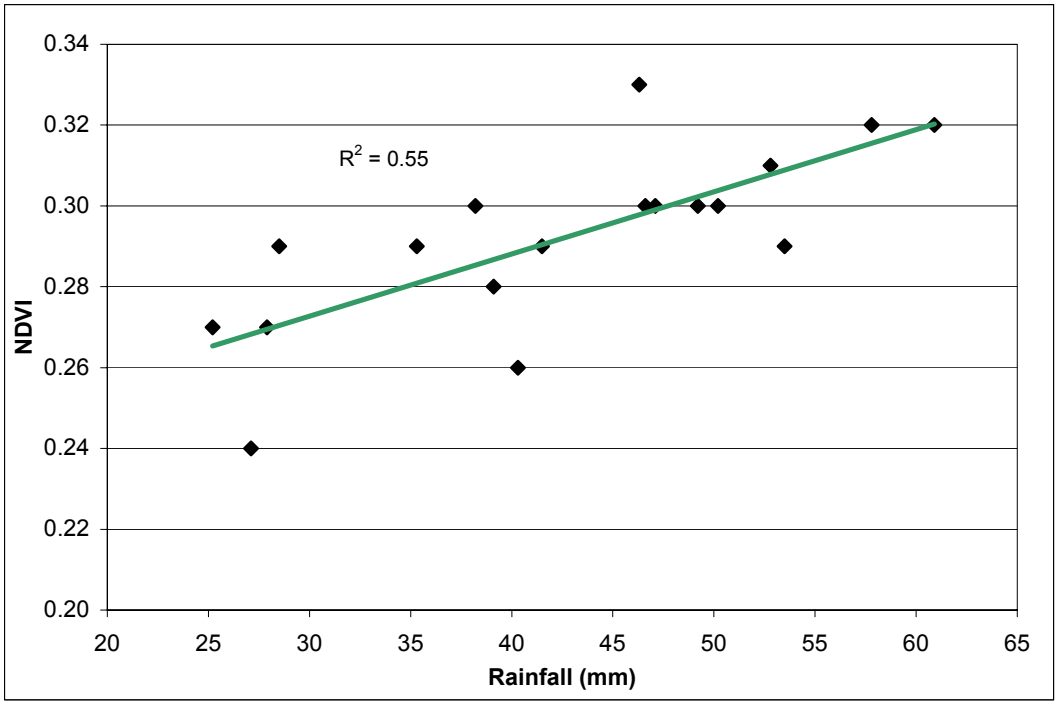

Figure 4.8. NDVI-precipitation scatter plot for study site 1A located in the Sudan.

The relationship between NDVI and rainfall for study site 3A located in southern Mauritania was weak and not significant with $R^2 = 0.19$, and $P = 0.065$.

4.4 Visual analysis

Change in land cover was determined by computing the differences in land cover and land use statistics over the time period. Overall change from one land cover and land use in 1984 to another in 1999 was as well calculated. This was determined by simple pixel-to-pixel comparison resulting in a land cover change matrix, which displays the proportion of each element in 1984 that changed to another class in 1999, thus, diagonal values are land cover or land use proportions that did not change between the studied years. Land cover change matrices are displayed in Appendix.

As can be seen in Figure 4.9, study site 1A is mostly covered by grassland, as this class-category constituted approximately 56.3 % of the total area in 1984 and 38.4 % of the total area in 1999. Open shrubs occupied 21.4 % in 1984 and 30.1 % in 1999 while closed shrubs covered 1.1 % of the area 1984 and 8.1 % 1999. The class open trees and herbaceous vegetation did not differ as much as the other three classes between the two studied years, covering about 21.1 % and 23.5 % of the total area in 1984 and 1999 respectively.

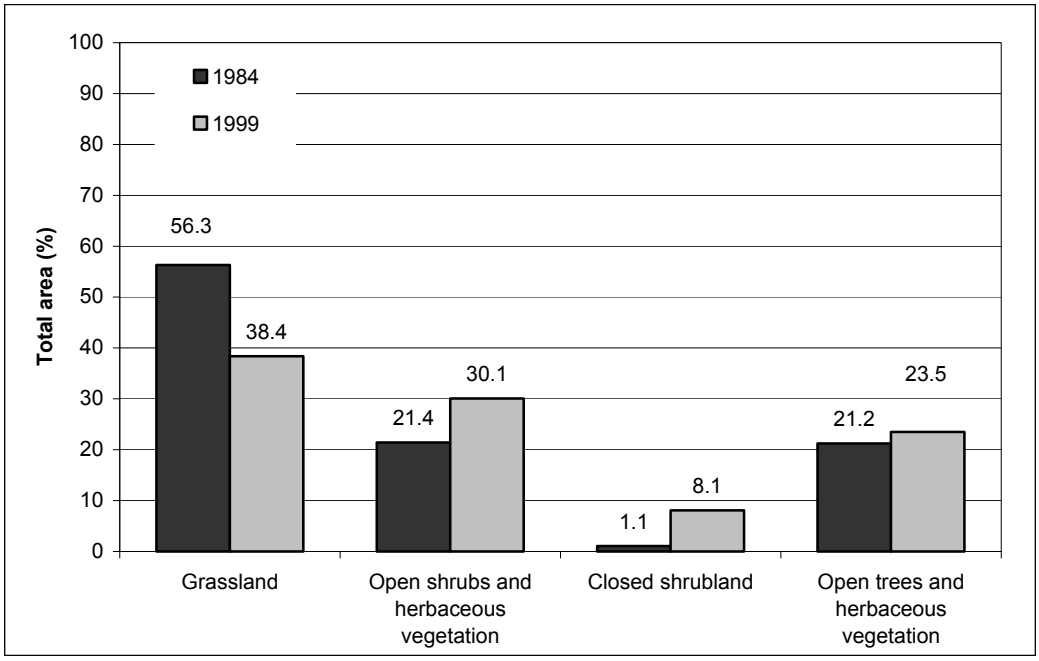

Figure 4.9. Land cover of total area for study site 1A, located in the Sudan. Black columns = 1984, grey columns = 1999.

Study site 1B showed signs of containing burnt areas before the acquisition of the Landsat 5 TM image, 24.3 % of the area was thus interpreted as a burnt scar. Vegetation in the area had regenerated in the 1999 image. No clear signs of human activity were to be found in the Sudan study sites 1A and 1B. However, in study site 1C (Figure 4.10), large regularly patterned patches interpreted as grazing land interspersed with crops was

found. These patches occupied approximately 17.8 % of the total area at the year 1984 and had increased to 23.6 % of the total area in 1999.

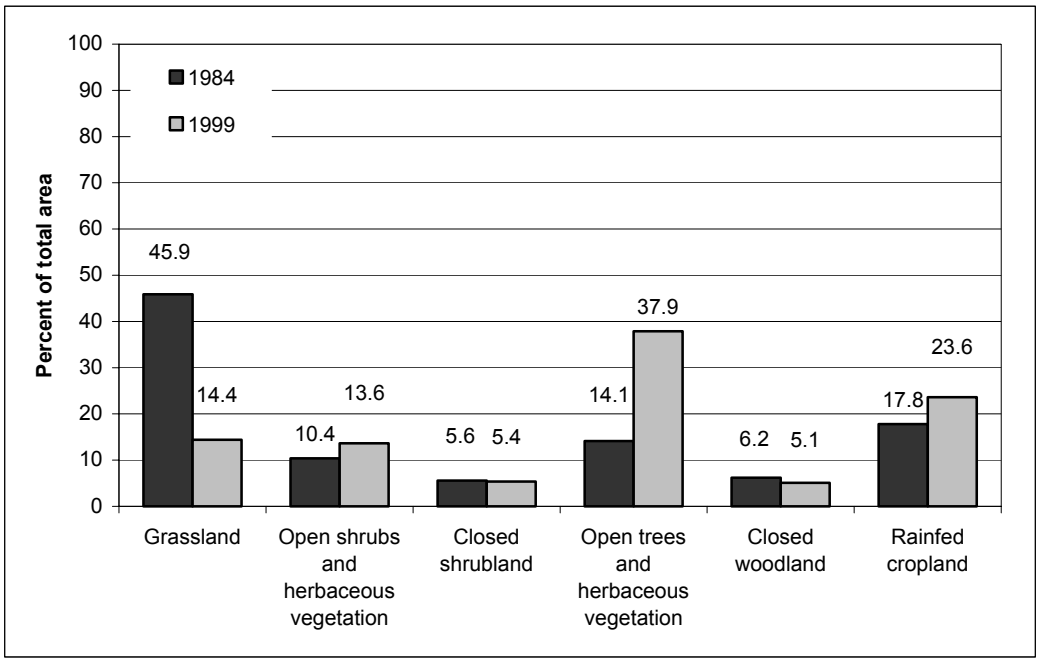

Figure 4.10. Land cover of total area for study site 1C located in the Sudan. Black columns = 1984, grey columns = 1999.

For study site 2A (Figure 4.11), vegetation between the years did not differ as much except for a belt around the tributaries of a river running through the locale. It was observed that small forest areas within this site had been cleared. This could either have been done as wood extraction for domestic uses, or in order to make space available for more crops. As a consequence, irrigated cropland had increased from 5.3 % of the total area in 1984 to 13.0 % of the total area in 1999.

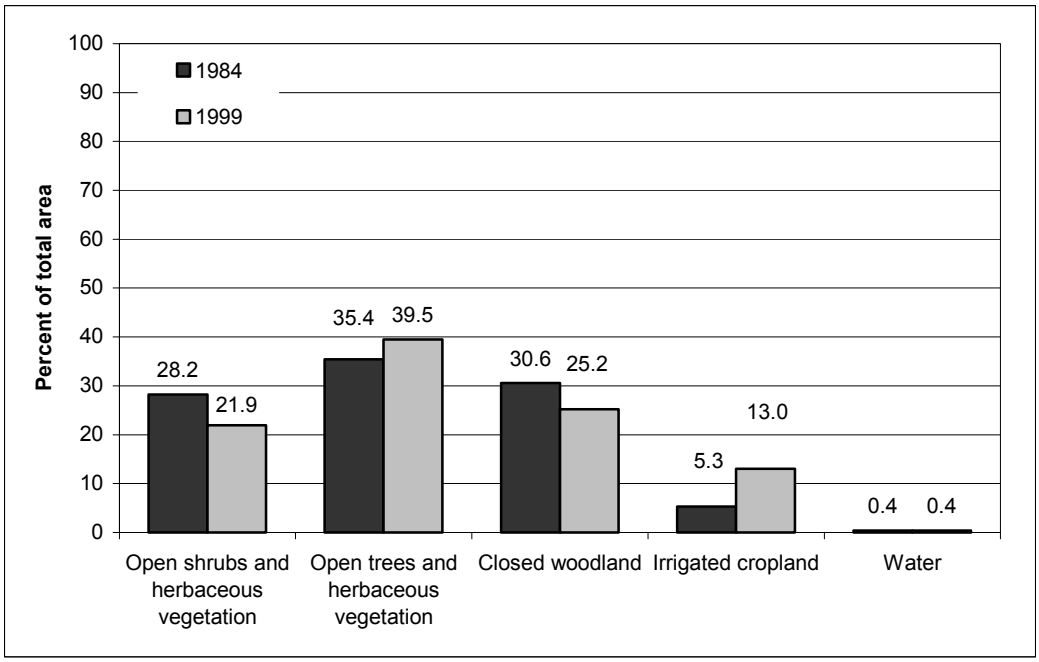

Figure 4.11. Land cover of total area for study site 2A located in the C.A.R. Black columns = 1984, grey columns = 1999.

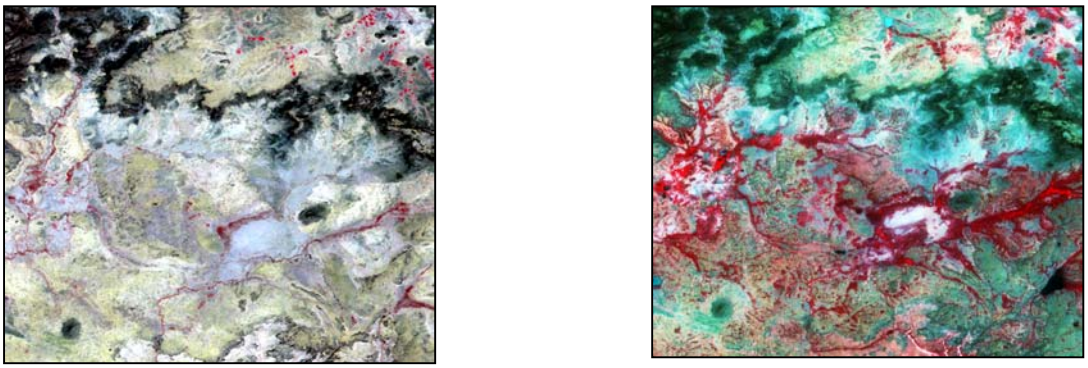

Figure 4.12. Landsat 5 bands 4, 3, 2 acquired October 1984 to the left and Landsat 7 bands 4, 3 and 2 acquired October 1999 to the right for Mauritania study site 3A. Difference in the amount of herbaceous and shrubby vegetation between the two dates is evident.

The difference in vegetation pattern in the Mauritania and Sudan sites between 1984 and 1999 was evident. These sites appeared severely desiccated in 1984 as compared to 1999. The apparent difference for study site 3A can be seen in Figure 4.12, with left image showing Landsat TM bands 4, 3 and 2, acquired October 21st 1984, and the right image showing Landsat ETM+ bands 4, 3 and 2 October 7th 1999. Figure 4.13 shows land cover statistics for the same area. It was observed that the amount of barren or sparsely vegetated areas was less in 1999 than in 1984 covering 52.5 % and 88.3 % respectively. As a result, probably due to more intense rains, a higher amount of shrubby and herbaceous vegetation was found in the 1999 Landsat imagery.

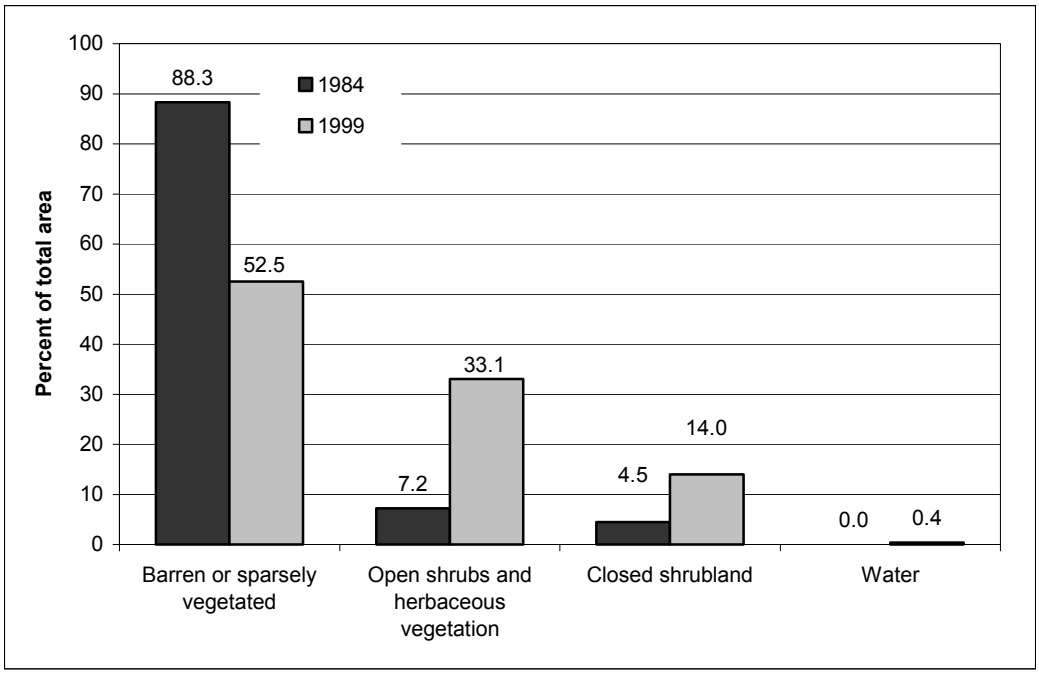

Figure 4.13. Land cover of total area for study site 3A, located in Mauritania. Black columns = 1984, grey columns = 1999.

4.5 Change vector analysis

Images resulting from the CVA represent the phase angle clockwise from north. The phase angles are described by colour type. A 0˚ or 360˚ angle indicates a pure increase in greenness while a 180˚ direction is pure decrease in greenness. An angle of 90˚ indicates a pure increase in brightness while an angle of 270˚ is a pure decrease. Along these four axes the major types of land cover change generally can be described; (i) decrease in wetness, towards the far left of the colour bar between 0˚ and 90˚; (ii) increase in wetness, indicated by angles varying between 180˚ and 270˚. These two are principally based on the fact that increased water content would cause a decreased signal in the greenness and brightness indices, and vice versa for angles located between 0˚ and 90˚. This is however not a matter of fact, as other factors may contribute to an increase or a decrease in both indices; (iii) An increase in vegetation is on the far right with angles varying between 270˚ and 360˚ while; (iv) a decrease in vegetation is represented by angles from 90˚ to 180˚.

Figure 4.14 show the results of the CVA over study site 2A, a no significant NOAA NDVI trend area (Eklundh & Olsson, 2003). It can be noted that the occurring angles mostly are located within the third quadrant, thus, indicating increased wetness since 1984. However, it is important to state that the derived magnitude image show that these changes are minimal and could have been caused by the high amounts of rainfall received in 1999 compared to 1984.

Observe the small belt of changes stretching east to west, occurring in the first and fourth quadrant in the positive brightness section depicted in the image in yellowish and reddish colours. These changes have occurred in areas interpreted as a loss of woody vegetation in order to make land available, possibly for irrigated crops, along the banks of tributaries

to the Boungou River running through the site. This makes sense, as clear-cutting results in more bare soil exposed (more brightness and less vegetation). Not surprisingly, the derived magnitudes are higher in these areas than changes in other quadrants.

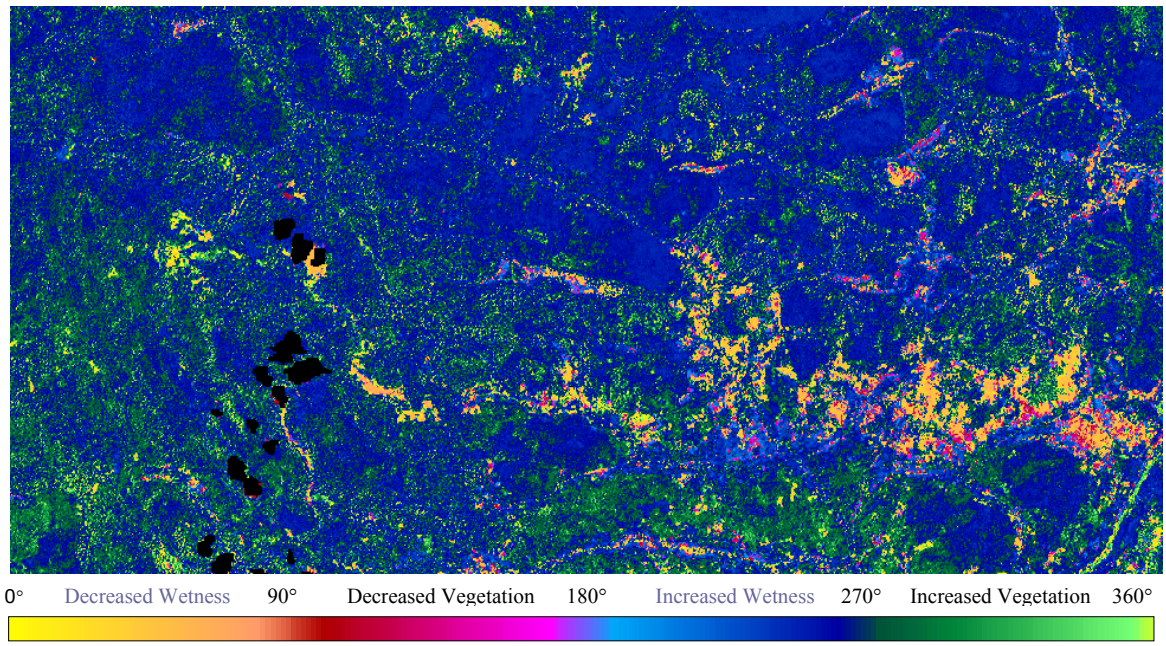

Figure 4.14. Change vector analysis image from November 1984 to November 1999 for study site 2A located in the C.A.R. A 0˚ or 360˚ and 180˚ angle indicates positive or negative greenness change. A 90˚ and 270˚ angle indicates change in either a positive or negative brightness direction.

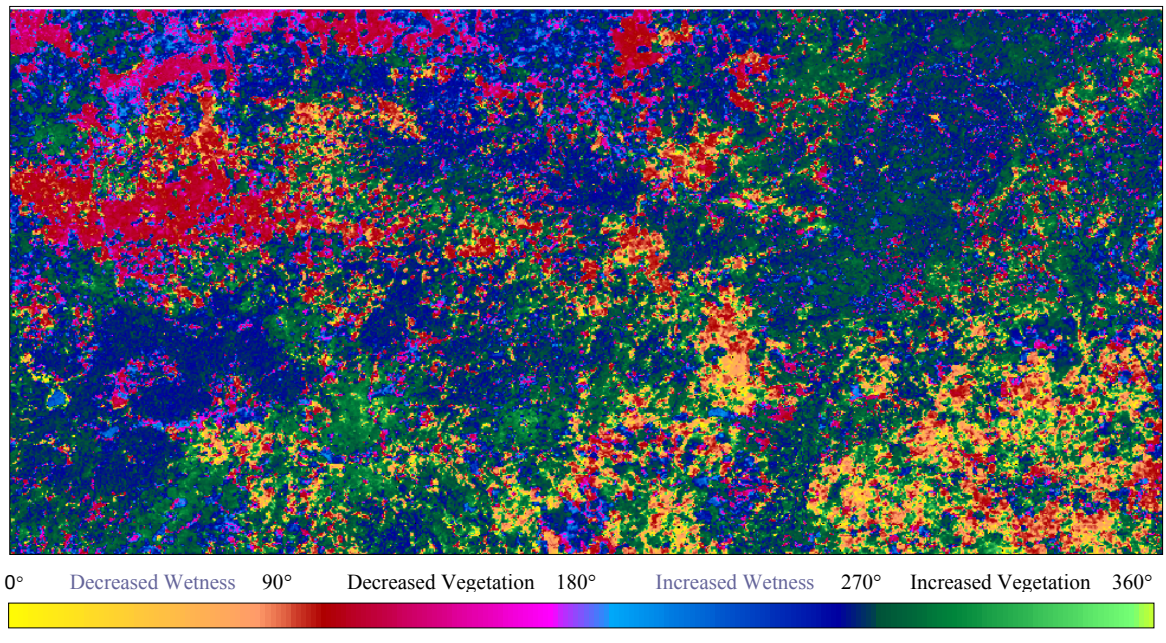

Figure 4.15. Change vector analysis image from September 1986 to September 1999 for site 4B located in Niger. A 0˚ or 360˚ and 180˚ angle indicates positive or negative greenness change. A 90˚ and 270˚ angle indicates change in either a positive or negative brightness direction.

Areas with a strong positive trend in NOAA NDVI, according to Eklundh & Olsson (2003), showed signs of having larger amounts of areas with an elevated active greenness compared to sites with a no significant trend in NOAA NDVI. Figure 4.15 and 4.16 shows the CVA method put into practice for study site 4B and study site 4A. In Figure 4.12 a 0˚ or 360˚ angle indicates that almost all land cover change is in the positive greenness direction. It is clear that most pixels have undergone change in the second quadrant, thus indicating an increase or a difference in greenness or vegetation activity and a decrease in brightness. Study sites 1A 1B, 1C and 3A show the same patterns as the figure below, with a considerable amount of change pixels localized somewhere between 270˚and 360˚.

Towards the northwest in figure 4.16, a meandering pattern with and almost pure increase in greenness can be seen on edge slopes. This increase as well as the small areas with a decrease in vegetation was confirmed upon visual comparison between the Landsat TM and ETM+ subsets.

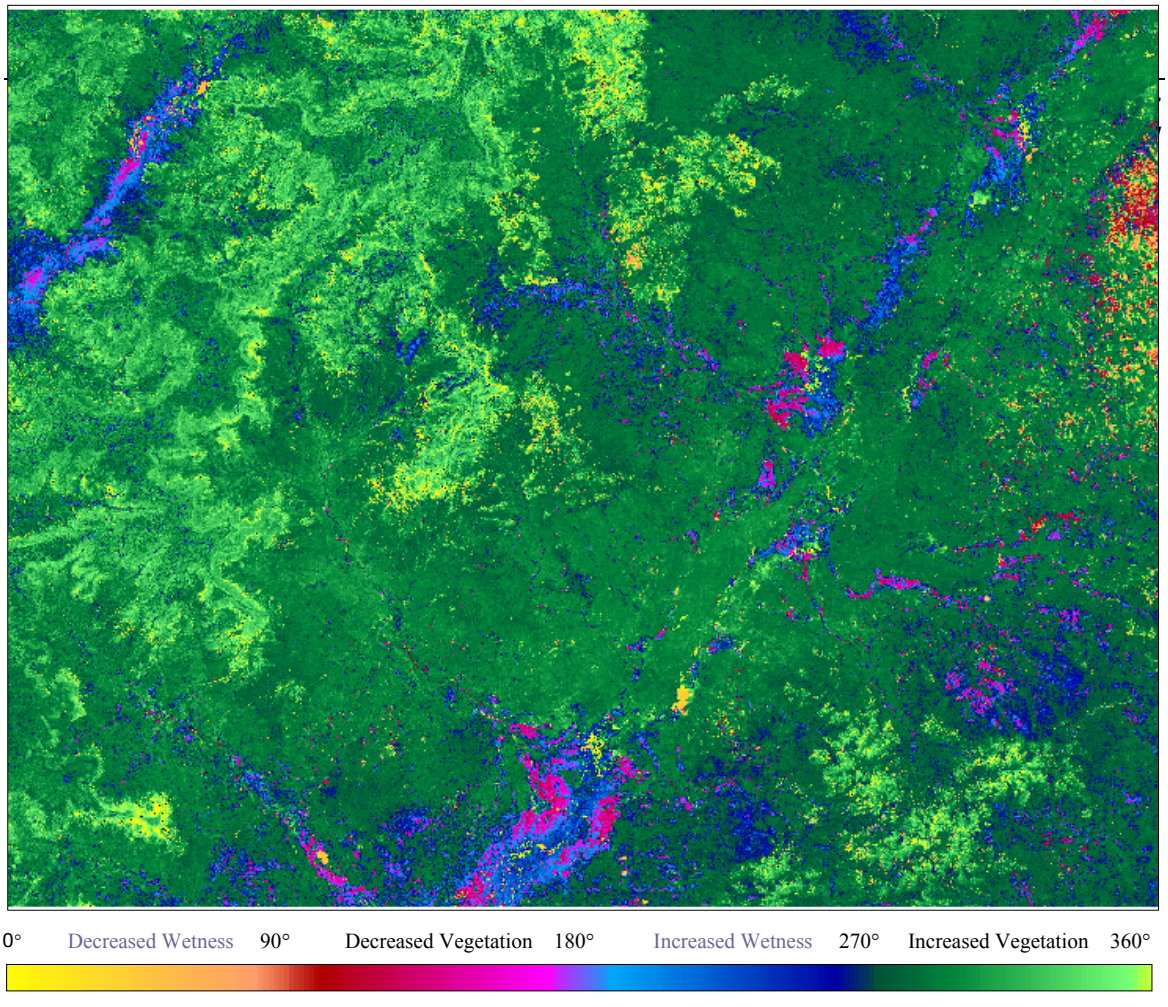

Figure 4.16. Change vector analysis image from September 1986 to September 1999 for site 4A located in Niger. A 0˚ or 360˚ and 180˚ angle indicates positive or negative greenness change. A 90˚ and 270˚ angle indicates change in either a positive or negative brightness direction.

It was observed that study site 4B had 16 % more of its pixels located between angles 90˚ and 180˚ and 22.1 % less of its pixels located between angles 270˚ and 360˚ than study site 4A. This is noticeable in Figure 4.17 showing images representing clusters of change. In the left hand side image, a high frequency cluster between angles 270˚ and 360˚ can be seen while on the right hand side, frequencies vary more with two mid and high frequency clusters located within 90˚-180˚ (decreased vegetation) and 260˚ to 360˚ (decreased wetness, increased vegetation).

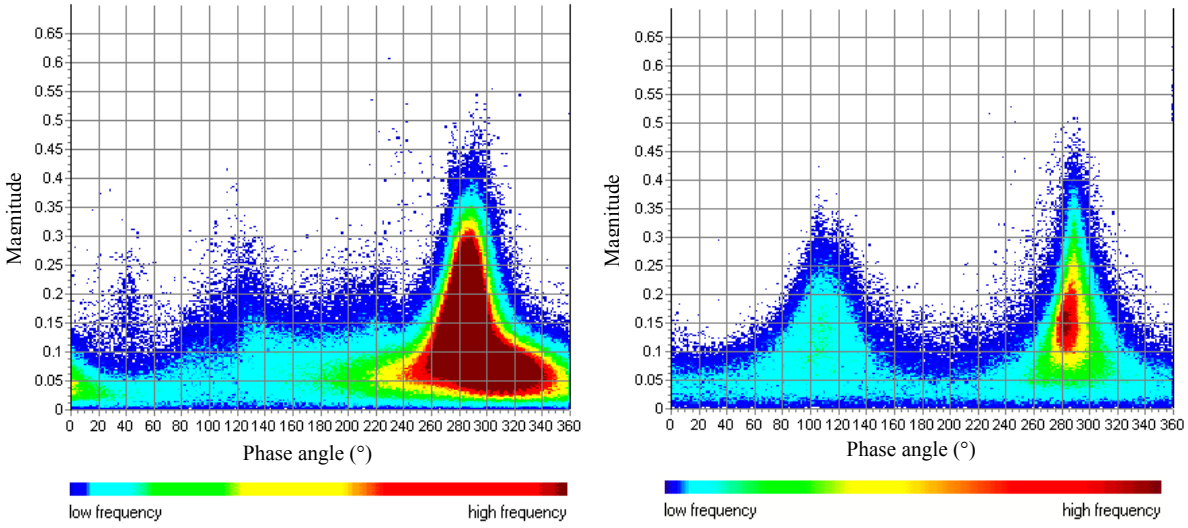

Figure 4.17. Magnitude against phase angle plot for the two study sites. Left hand side; Study site 4A. Right hand side; Study site 4B. One can identify clusters of change. X-axis = phase angle, Y-axis = magnitude.

4.6 NOAA and Landsat image comparability

Monthly mean intervals of NOAA NDVI images were used for comparison to locate the Landsat TM and ETM+ images in the vegetation cycle in order to evaluate the seasonal point for each image.

Figure 4.18. shows this method put into practice for the study site 1A, thus, Landsat TM and ETM+ WRS-2 path/row 179/52. The diurnal rainfall pattern between the two years is different, as the area received significantly more rainfall during 1999 than in 1984. This in turn, possibly led to significantly higher values of NDVI, thus, to some extent explaining the results derived from the interpretation and the CVA. The images fit well with the NOAA NDVI for the November month but the difference between the images due to different climatic conditions that preceded the recording of the imagery is evident.

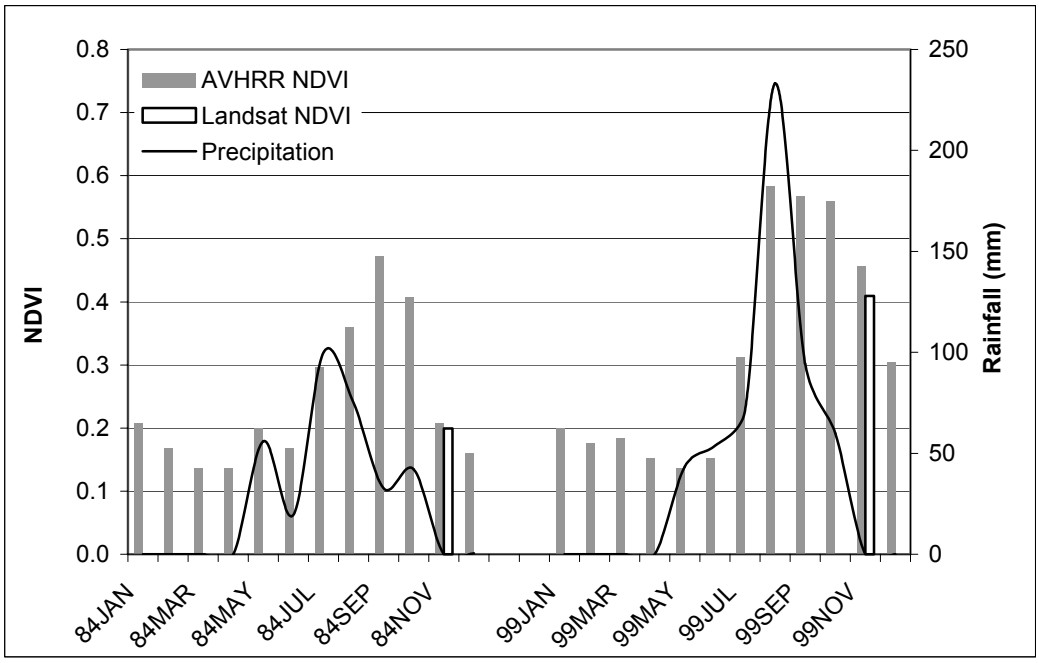

Figure 4.18. NDVI, rainfall (mm) comparison between the year 1984 and 1999, Southern Kordofan district, Central Sudan. Climate data derived from nearest ground station, Er-Renk (the Sudan).

Figure 4.19 shows a comparison between AVHRR, Landsat TM and ETM+ for study site 2A. The total amount of rainfall during 1984 is less than 1999 but this appears not to have had an effect on NDVI over the area. Rainfall pattern is quite similar between the two years, except for August and September where rainfall in 1999 exceeded 1984. Selected Landsat TM and ETM+ pixels are almost a perfect match in the NOAA AVHRR time series.

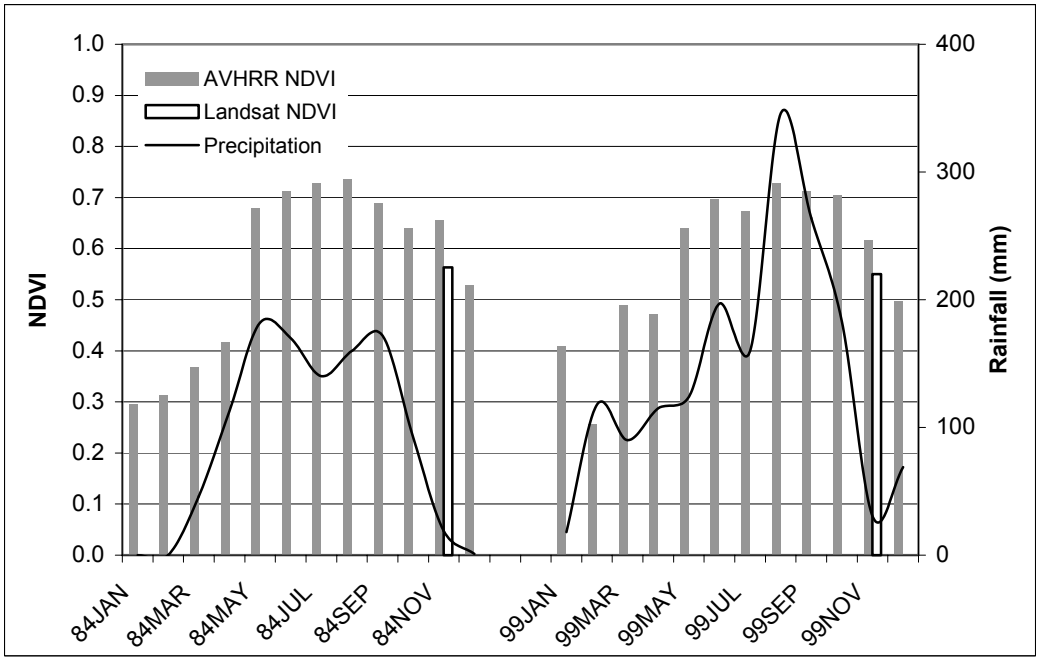

Figure 4.19. NDVI, rainfall (mm) comparison between the year 1984 and 1999, Hautte Kotto, central C.A.R. Climate data derived from nearest ground station, Bria. (C.A.R.)

Figure 4.20 shows a comparison between AVHRR and Landsat TM and ETM+ over site 3A. Mean rainfall values have been employed for June and August for the year 1999 respectively as these were unavailable in the original dataset for that year. Precipitation following the September month dive sharply in both years. One can notice that the Landsat TM NDVI value is higher than its NOAA AVHRR counterpart, in contrast, the Landsat ETM+ NDVI value fits very well.

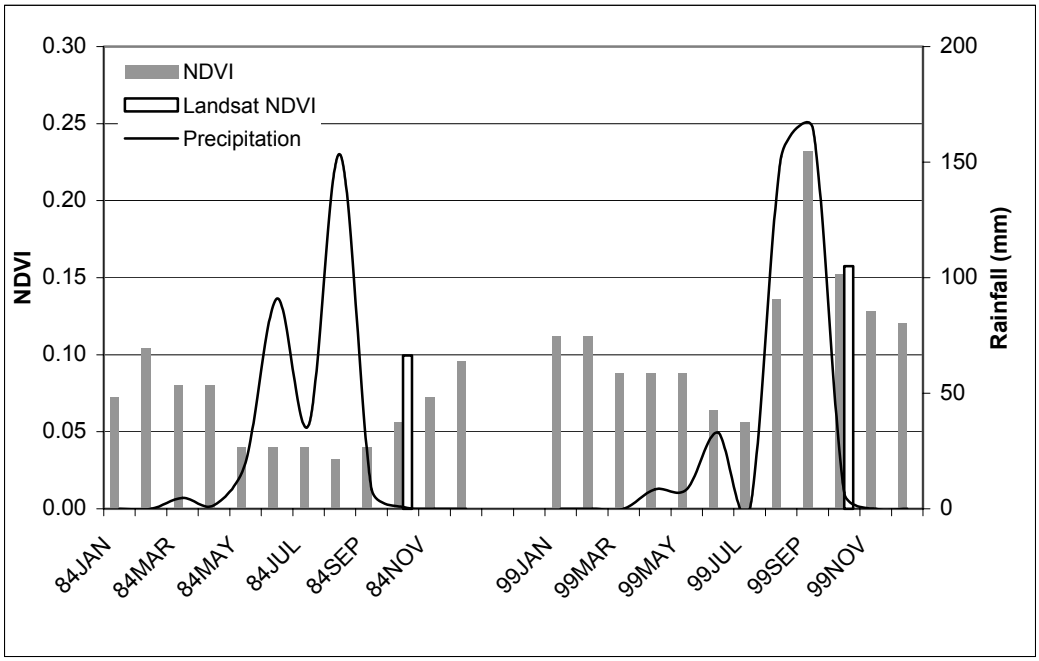

Figure 4.20. NDVI, rainfall (mm) comparison between the year 1984 and 1999, Hodh El Gharbi, Southern Mauritania. Climate data derived from nearest ground station, Nioro Du Sahel (Mali).

4.7 Summary of results

1. Trend analysis shows that both rainfall and NDVI have increased for study sites categorized as significantly strong positive according to Eklundh & Olsson (2003). The magnitude of these positive trends on the other hand varies. Data trends begin with a number of years with exceptionally low values and no account has been taken to the beginning and end of the growing season.

2. Values for annual rainfall compared to annual NDVI is significantly but weakly correlated ($R^2 < 0.6$ at $p < 0.05$). The strong trend in NDVI can thus only partly be explained by an increase in rainfall.

3. Visual analysis shows that differences between the years 1984 and 1999 in land-cover exist, generally extensive over areas located in the Sudan and Mauritania with, according to Eklundh & Olsson (2003), a strong positive trend in NDVI. For these sites, a transition from generally barren land or sparse herbaceous vegetation was observed, as well as regeneration of vegetation due to fires.

4. The CVA illustrate that selected sites in the Sudan, Niger and Mauritania with a significantly strong positive change in NOAA NDVI typically had pure 270˚-

360˚ angles indicating that almost all change is in the positive greenness direction. This could indicate an increase in vegetation during the time period. In comparison to sites with, according to Eklundh & Olsson (2003), a strong positive trend in NOAA NDVI no trend areas had lower magnitude values while phase angles varied more within the 0°-360° angular range.

5. Image comparability shows that Landsat TM and ETM+ scenes in most studied cases fit well with the NOAA AVHRR time series. However it is clear that phenological differences, probably due to different climatic conditions, exist. This in turn could have lead to amplifications of the observed differences in vegetation activity derived from the visual analysis and CVA.

5 Discussion

5.1 Satellite imagery and methodological discussion

5.1.1 Landsat data

The analysis of land-cover change using multitemporal Landsat data is complicated by the presence of substantial radiometric differences (Yuan & Elvidge, 1996; Markham and Barker, 1986), and one can not eliminate the possibilities that variations in the radiometric characteristics between TM and ETM+ scenes due to for example sensor performance, climatic conditions and cloud/shadow effects have arisen.

In a perfect remote sensing system, all images in a time series can be corrected for atmospheric and illumination effects and calibrated for surface reflectance factors for direct comparison but this is an almost impossible goal, and one can only hope to minimize the negative effects. However, by converting Landsat 5 DNs to 7 DNs followed by a digital number conversion from both sensors to radiance and then at-satellite reflectance, a large part of the impact due to instrument related artifacts and sun illumination geometry has been reduced. Despite the fact that Lu et al. (2004) state that it is important to use the same sensor, studies carried out by Vogelmann et al. (2001) show that Landsat 5 and Landsat 7 data have until 1999 indicated a high degree of similarity, implying that investigations to measure and monitor landscape occurrences can be sustained with minimal caution even if Landsat 7 data are devoid of many of the instrument related artifacts that characterize Landsat 5 data.

The results of the AVHRR and Landsat image comparability show that divergence in phenological characteristics exist between the imagery, probably due to a difference in rainfall conditions preceding the recording of the images. The divergence in rainfall pattern for the sites located in Sudan and Mauritania were quite evident. And for these sites, one cannot rule out that this in turn could have led to an amplification of the results as an effect of exceptionally more favorable water conditions throughout the year 1999 than in 1984.

Moreover, it appears that the majority of the Landsat TM and ETM+ satellite images have values that are lower than their NOAA AVHHR NDVI counterparts. This could be due to the fact that spectral data between the sensors are captured differently with the NOAA AVHRR sensor collecting data with a wider spectral range in both the red and NIR channels. Stevens et al. (2003) compared vegetation indices from a wide range of different sensors, including TM, ETM+ and AVHRR, and state that the greatest departure of ideality occurs with the AVHRR if narrow band values, such as the TM and ETM+, are taken to represent the ideal vegetation index. Atmospheric factors, such as water vapour, which reduces the NIR reflectance observed by the satellite, as well, has a significant impact on the AVHRR channel 1 and 2 data, negatively biasing the AVHRR NDVI.

To minimize the temporal framework and the effect of fluctuating rainfall regimes it would have been useful with at least one or two high-resolution images in-between the analyzed years. No in-between images were however found in the GLFC image database and acquiring such an image or images outside this record would have been too expensive for this project.

5.1.2 NOAA data

Known inaccuracies for the AVHRR sensor arise from orbital drifts, coarse resolution, lack of onboard calibration capability for the visible and near infrared channels, and their wide spectral bandwidths. All these effects can contribute and increase the interference with the surface signal and the variation in sun-target-view angles.

As the time in orbit for the NOAA satellites increases, illumination conditions are changing with time from launch with NOAA satellites affected by approximately 30 min delay in orbital crossing time annually (Eklundh & Olsson, 2003). The satellites lack any active orbital adjustment capability, leading to later overpass times as the orbit degrades itself. This in turn, lead to systematic shifts in Solar Zenith Angle (SZA) with reflectance values being affected by a combination of absorption and scattering in the atmosphere and according to Los et al. (2000) tends to decrease NDVI over vegetated surfaces. Kaufmann et al. (2000), however, investigated the influence of SZA on NOAA PAL NDVI concluding that the differences with changes in SZA are primarily a soil–induced effect with the strength depending on the reflecting surface. Thus, the effect of SZA on NDVI will decrease as leaf area in the canopy increases, darkening the ground under the canopy. Areas that have high NDVI values are therefore minimally influenced by changes in SZA.

Since composite images are a mosaic of pixel measurements obtained at different dates and with varying viewing geometries, the algorithm to select each composite pixel is of importance (Cihlar et al., 1994). MVC compositing reduces cloud influences for a range of viewing and illumination angles and for all aerosol conditions (Holben, 1986). However, positively biased noise may arise due to the spatial and temporal compositing of the data. As for example, burning of vegetation reduces the NDVI signal, the maximum NDVI approach will thus select a pixel prior to the fire if it chooses between two or more images with comparable atmospheric and viewing conditions (Barbosa et al., 1998). Similarly, the MVC procedure will preferentially select vegetated pixels over spatially adjacent non-vegetated pixels. Boundaries of vegetated areas will thus be enlarged, causing non-vegetated areas to shrink or disappear (Roy, 2000).

Problems with satellite shifts have as well been mentioned as the times series is composed of data from four satellites, NOAA-7, -9, -11 and –14. Efforts by Kaufman & Holben (1993) have been dedicated to this and most of these errors seem to have been removed during processing of the Pathfinder AVHRR Land dataset (Prince & Goward, 1996; Kaufmann et al. 2000). Slayback et al. (2003) reported no trends, for mid and high latitudes, for individual satellites or across the time period for the GIMMS data set, indicating the success of calibration and intercalibration between data from the NOAA-7, -9, -11 and -14 satellites. However, they noted decreasing trends for individual satellites at low latitudes and concluded that these changes do not reflect changes in land surface or atmosphere, rather, trends reflect changes in viewing or illumination conditions.

5.1.3 Change detection techniques

Deane et al. (1986) stressed the importance of choosing the right interpretation approach when using satellite imagery, reporting that visual interpretation of high-resolution remote sensing data often is accurate used appropriately. The visual analysis process was made relatively simple with a multi-window approach with frames containing essential

information as support. Nevertheless, with this information primarily based on ancillary data with the likes of past land cover or land use data and as no ground truth data were used it can be discussed whether the derived results are accurate and reliable. The accuracy concerning the additional data is occasionally described vaguely or in complex terminology.

The following uncertainties may have contributed to the wrong assignment of class labels in the visual analysis; (i) classes are not, and should not be considered pure, but mixtures of land cover with the class name corresponding to the dominant covers present; (ii) the use of a variety of ancillary data introduces the problem of multi-source and multi-date data integration; (iii) land use and land cover classes are based on remotely sensed land use and land cover characterisations and can, as a result, at best have the same accuracy; (iv) land cover with herbaceous vegetation and no clear field boundaries introduce uncertainties and make them difficult to map when land use related to a field pattern tend to concur with an identified land cover; (v) uncertainties as to how much of the land use areas designated as cropland are actually used to grow crops, as other agricultural infrastructures of land was included; (vi) uncertainties concerning areas mapped as cultivated rainfed, these may include irrigated practices not dependent on closeness to water, such as ground water irrigation.

It is possible that errors of overestimation/underestimation have occurred during delineation in the visual analysis, however, these errors may be relatively constant at both years, making the observed changes adequately accurate. As the process of visual analysis is time costly and as it is difficult to estimate trajectories of change detection, accuracy was thought to be improved by combining the results from the visual interpretation with a digitally based change detection method. For example, woodland logging or other disturbances usually are difficult to detect using computer processing, however, visual interpretation has the potential to identify such changes. Previous research has shown that a combination of two change detection techniques could improve the change detection results (Lu et al., 2004).

Sohl (1999) concluded that the CVA method excelled at producing rich qualitative information about the nature of change in comparison to “enhanced” image differencing, vegetation index differencing and post-classification differencing, and Johnson & Kasischeke (1998) summed up the potential advantages. A problem must however be elevated, namely the predicament of applying a threshold for the end results, a known difficulty for many change detection algorithms. In several studies a threshold of 2 standard deviations from the mean has been applied for the CVA. This approach has however been deemed as scene dependent (Lu et al., 2004). Even though a number of advanced techniques have been developed, they are usually complex, and as the CVA method itself was relatively time consuming, none of these threshold methodologies was implemented.

Accuracy assessment is of very high importance when dealing with land use change studies and requires the sampling of a statistically significant amount of pixels. The lack of reliable field-based datasets prevented the making of a quantitative analysis of the research results. A degree of carefulness regarding the quantitative results is thus justified.

5.2 End result discussion

Widespread degradation of the Sahel is generally treated as an established fact and there are evident cases of local degradation in the Sahel (Prince et al. 1998). However, as mentioned earlier, this view has been challenged and Prince et al. (1998) argues that the local scale has often generally been considered and should by no means be extrapolated to the whole of the Sahel.

Rasmussen et al. (2001) observed a partial recovery of both herbaceous and woody vegetation following severe reductions in vegetation cover during the 1970s and 1980s over parts of northern Burkina Faso, concluding that broad generalizations on land degradation processes based on local scale studies are risky. Eklundh & Olsson (2003) observed a geographically consistent pattern of increasing NDVI across the Sahel between the years 1982 and 1999. Prince et al. (1998) concluded that no extensive degradation of the Sahelian zone could be detected as small but significant upward trends in Rain Use Efficiency (RUE), the ratio of Net Primary Productivity (NPP) to precipitation, was observed over the same region between the years 1982 and 1990. Nicholson et al. (1998) found no evident progressive change in either the desert boundary or the vegetation cover in the Sahel during 1980-95. All these studies may be said to support the "new paradigm" as Rasmussen et al. (2001) put it, according to which arid environments are seen as highly variable, "event-driven" systems rather than equilibrium systems.

The visual analysis and the CVA resulted in an estimated deviation or increase in land cover for the sites located in the Sudan, Niger and Mauritania, classified as statistically significant strong positive in NOAA NDVI and a decrease or no noteworthy change in land cover for the selected sites classified as no statistically significant change in NOAA NDVI. Through the results a number of general processes of land cover change could be noted; (i) a significant increase in greenness and a significant decrease in brightness over extensive areas indicating a divergence or a recovery in land cover due to difference in rainfall amount, difference in rainfall regime or other unnoticed effects; (ii) probable land modifications characterized by a divergence or a recovery in land cover generally distinguished by a transition from herbaceous or sparse vegetation to woody vegetation due to difference in rainfall amount, difference in rainfall regime or other unnoticed effects.

"Unnoticed effects" could be accounted for by phenomena, which due to either lack of time or data (intricate local knowledge) have not been included in this study, such as: (i) Variations with type of land management and livestock activities; (ii) Variations in population changes, thus, transformations in for instance input labor and market participation. For example, Rayanaut (2001) point out that the Sahel presents enormous demographic variability and concluded that areas with the least arid climate and best soils are not the mostly populated, rather, settlement patterns have much more to do with history; (iii) Variations with terrain or soil type, as for example vegetation on sandy soils is consistently greater and may recover earlier after rainfall than clay soils due to higher infiltration rates (Kumar et al., 2002).

5.2.1 Effect of rainfall

Through regression analysis it was observed that annual rainfall compared to annual NDVI was significantly but only weakly correlated for 5 of the 6 tested sites. For 3 out of the 4 areas with, according to Eklundh & Olsson (2003), a significantly strong positive trend in NOAA NDVI the relationship was significant. For one site annual rainfall and annual NDVI was not well correlated, this could imply that a positive change in vegetation is due to other factors than increasing rainfall. It is however very important to note that the rainfall data used for this site was collected from a climate station approximately 90 km away from the analysed area, thus, being a large factor of uncertainty possibly resulting in the poor correlation. It is also important to note that the integration of rainfall values annually could have caused a poor correlation as not only total annual precipitation but also the intensity of single rainfall events play an important role in the occurrence of vegetation (Tucker, 1991).

Rainfall can certainly said to be one of the causes of a possible vegetation increase, as a recovery from the severe droughts of the early 1980s has been observed (Hulme et al. 2001), however, implying that this is the only factor involved may be a simplification, as change is possibly due to the effect of a combination of driving forces as contrasts among local areas often are extremely diverse. Graef & Haigis (2001) for instance showed that annual differences of 200 – 300 mm of rainfall may occur within a radius of only 100 km. Making a simple comparison between NDVI and precipitation, thus, requires local knowledge of the variability of these two. The spatial resolution of 8 km of NDVI and the regional rainfall data used is, thus, an apparent problem when relating rainfall and vegetation trends. Diouf & Lambin (2001) recognizes this, as they found a statistical significant, but not very strong relationship with R^2 values equaling 0.41 at a local scale, emphasizing that rainfall at a regional scale may control a large part of the spatial and temporal variation in vegetation cover compared to the local scale where responses of vegetation to rainfall may vary more.

5.2.2 Agricultural management

As the Niger study sites contained a large amount of agricultural fields of which, according to the change vector analysis, have undergone vegetation increase, one should dig deeper into the agricultural practices evoked at these sites and investigate possible reasons for the increase in greenness and NDVI. One possible explanation could be a difference in the amount of fields cultivated. In order to sustain self-sufficiency farmers could be forced to cultivate fallow land or clear new fields and take them under cultivation because of food shortages. Wezel & Haigis (2002) carried out a survey in 136 farm households from seven villages located in southern and central Niger. Most farmers mentioned that they had more fields under cultivation than fallow land from the mid 1980s on to present time. It is not intuitive however that all cropped areas show higher greenness or NDVI (depending on density, type of crop and temporal growing pattern) than fields that are left fallow, but this could certainly be the case as according to Uchida (2001) who, in an attempt to discriminate agricultural land use in semi-arid Burkina Faso, mention that rain fed cropped areas had as high NDVI values as dense vegetation during the crop growing period. However, to fully evaluate this statement, detailed studies are needed in order to assess the temporal profiles as well as the precise amount of areas under cultivation and fallow. It should be noted, that if this is the case, decreased areas

under fallow is not beneficial in a long-term perspective, as they are crucial for soil fertility management (Wezel & Haigis, 2002).

5.2.3 Species composition

An increasing trend of NOAA NDVI and a difference in greenness could also indicate a change in vegetation type. It has been shown that species show inter-annual fluctuations in its occurrence in the Sahel, as for instance Wezel & Schlecht (2004), who monitored fallow plots in southwestern Niger during 3-5 years and noted that many different species were present in some years but absent in others. In addition to this, Karnieli et al. (2002) studied the seasonal vegetation dynamics over two years in a semi-arid environment and concluded that the temporal analysis of natural vegetation should take into account the difference in annual NDVI signals between perennial and annual species. Perennial vegetation exhibits different spectral responses throughout the year while annual plants are green only for a relatively short period of time. An increasing trend of NOAA NDVI, thus, may well not only be due to an increase in vegetation productivity, but also a change in annual and perennial species composition, which in turn, could result in an increasing trend of the NOAA NDVI amplitude.

6 Conclusion

In this study temporal trends in NDVI and rainfall were investigated as well as spatial trends by implementation of change vector analysis and visual interpretation of high-resolution imagery. Here follows a summarization of the observations made.

- Trend analysis show that NDVI has increased for study sites categorized as significantly strong positive by Eklundh & Olsson (2003). Positive significant slopes indicate an increase in NDVI throughout the time period for five out of seven studied sites.

- Trend analyses show an increase in rainfall with positive slopes according to the linear trends.

- Annual rainfall and annual NDVI were only weakly correlated and significant for five of the six sites on which the analysis was carried out, indicating that rainfall is not the sole effect behind an increase in vegetation activity.

- Results of the visual interpretation of high-resolution imagery show a recovery in vegetation over areas with a significantly strong positive trend in NOAA NDVI.

- Phase angles and change magnitudes derived from the change vector analysis clearly differ between different NDVI trend study sites. Moreover, change vector analysis illustrate that land cover change for areas with, according to Eklundh & Olsson (2003), a strong positive trend in NDVI was in a positive greenness direction. This supports the results derived from the NDVI trend analysis and visual interpretation.

- Phenological differences between high-resolution satellite imagery exist, most likely due to different climatic conditions preceding the recordings of the imagery. A degree of caution is thus advised, as differences in rainfall pattern between studied years exist.

The derived results support a conclusion that studied areas with a strong positive trend in NOAA NDVI are greening. However, causes behind this greening are difficult to ascertain, as results show that increasing rainfall is not the only factor involved with values for annual rainfall compared to annual NDVI being significantly but weakly correlated. Change, is rather believed to have been caused by a combination of driving forces.

7 References

Agnew C.T., Chappell A., Drought in the Sahel, *Geo Journal, 48,* pp. 299-311, 1999

Ayoub A.T, Land degradation, rainfall variability and food production in the Sahelian zone of the Sudan, *Land Degradation & Development, 10,* pp. 489-500, 1999

Barbosa P.M., Pereira J.M.C., Grégoire J-M., Compositing criteria for burned area assesment using multitemporal low resolution satellite data, *Remote Sensing of Environment, 65,* pp. 38-49, 1998

Batjes N.H., Soil parameter estimates for the soil types of the world for use in global and regional modelling (Version 2.1; July 2002, ISRIC Report 2002/02c, *International Food Policy Research Institute (IFPRI) and International Soil Reference and Information Centre (ISRIC),* Wageningen, 2001

Campbell J.B., Introduction to remote sensing, 2nd edition, Taylor & Francis, London, 1996

Copans J., The Sahelian drought. In: Hewitt K., Interpretations of calamity. Allen and Unwin, London, pp. 83-99,1983

Crist E.P., A TM tasseled cap equivalent transformation for reflectance factor data, *Remote Sensing of Environment, 17*, pp. 301-306, 1985

Crist E.P., Cicone R.C., A physically-based transformation of thematic mapper data – the TM tasseled Cap, *IEEE Transactions on Geosciences and Remote Sensing, GE-22*, pp. 256-263, 1984

Deane G.C., Quegan S., Churchill P.N., Hendry A., Evans R., Trevett J.W., Land use feature detection in SAR images*, SAR applications workshop; proceedings of an ESA workshop*, pp. 95-102, 1986

Diouf A., Lambin E.F., Monitoring land-cover changes in semi-arid regions: remote sensing data and field observations in the Ferlo, Senegal, *Journal of Arid Environments, 48(2),* pp. 129-148, 2001

Eklundh L., Olsson L., Vegetation index trends for the African Sahel 1982-1999, *Geophysical Research Letters, 30(8),* pp. 13-1, 13-4, 2003

FAO, Food supply situation and crop prospects in Sub-Saharan Africa, 2001

FAO-UNESCO, Soil map of the world, 1997

Ford N., West Africa, *African Business, 294*, pp. 14-15, 2004

Gomes R., Petrassi F., Rainfall variability and drought in Sub-Saharan Africa, *FAO Agrometeorology series 9*, 1996

Graef F., Haigis J., Spatial and temporal rainfall variability in the Sahel and its effects on farmers management strategies, *Journal of Arid Environments, 48,* pp. 221-231, 2001

Helldén U., Desertification-time for an assessment, *Ambio*, 20(8), pp. 372-383, 1991

Holben, B.N., Characteristics of maximum-value composite images from temporal AVHRR data, *International Journal of Remote Sensing, 15*, pp. 33473363, 1986

Huang C., Wylie B., Homer C., Yang L., and Zylstra G., Derivation of a tasseled cap transformation based on Landsat 7 at-satellite reflectance, *International Journal of Remote Sensing, 23(8)*, pp. 1741-1748, 2002

Hulme M., Climatic perspectives in sahelian desiccation: 1973-1998, *Global Environmental Change, 11(1)*, pp. 19-29, 2001

Hulme M., Doherty R., Ngara T., New M., Lister D., African climate change: 1900-2100, *Climate Research, 17*, pp. 145-168, 2001

Josserand H., Aranda da Silva M., FAO/WFP crop and food supply assessment mission to Mauritania, *FAO Global information and Early Warning System on Food and Agriculture World Food Programme,* 2002

Justice C.O., Vermote E., Townshend J.R.G, Defries R., Roy D.P., Hall D.K., Salomonson V.V, Privette J.L., Riggs G., Strahler A., Lucht W., Myneni R.B., Knyazikhin Y., Running S.W., Nemani R.R., Wan Z., Huete A.R., Van Leeuwen W., Wolfe R.E., Giglio L., Muller J-P., Lewis P., Barsely M.J., The Moderate Resolution Imaging Spectroradiometer (MODIS): Land remote sensing for global change, *IEEE Transactions on Geoscience and Remote Sensing, 36*, pp. 1228-1249, 1998

Johnson R.D., Kasischke E.S., Change vector analysis: A technique for the multispectral monitoring of land cover and condition, *International Journal of remote Sensing, 19,* pp. 411-426, 1998

Jönsson P., Eklundh L., Seasonality extraction by function fitting to time-series of satellite data, *IEEE Transactions on Geoscience and Remote Sensing, 40(8)*, pp. 1824-1832, 2002

Kaufman Y.J., Holben B.N., Calibration of the AVHRR visible and near-IR bands by atmospheric scattering, ocean glint and desert reflection, *International Journal of Remote Sensing, 14*, 21-52, 1993

Kaufmann R.K., Zhou L., Knyazikhin Y., Shabanov N.V., Myneni R.B., Tucker C.J., Effect of orbital drift and sensor changes on the time-series of AVHRR vegetation index data. *IEEE Transactions on Geoscience and Remote Sensing, 38*, 2584-2597, 2000

Kauth R.J., Thomas H.S., The tasseled cap – a graphic description of the spectral-temporal development of agricultural crops as seen by Landsat, *Proceedings of the Symposium on Machine processing of Remotely Sensed Data,* Purdue University, West Lafayette, Indiana, pp. 4B41-4B51, 1976

Kumar L., Rietkerk M., van Langevelde F., van de Koppel J., van Andel Jelte., Hearne J., de Ridder N., Stroosnijder L., Skidmore A.K., Prins H.H.T., Relationship between vegetation growth rates at the onset of the wet season and soil type in the Sahel of Burkina Faso: Implications for Resource Utilization a Large Scales, *Ecological Modelling, 149*, pp. 143-152, 2002

Los S.O., Collatz G.J., Sellers P.J., A global 9-yr biophysical land surface dataset from NOAA AVHRR data. In: Slayback D.A., Pinzon J.E., Los S.O., Tucker C.J., Northern hemisphere photosynthetic trends 1982-99, *Global Change Biology, 9,* pp. 1-15, 2003

Lu D., Mausel P., Brondidízio E., Moran E., Change detection techniques, *International Journal of remote Sensing, 25*, pp. 2365-2405, 2004

Malila W., Change vector analysis: An approach for detecting forest changes with Landsat, *Proceedings, Machine Processing of Remote Sensed Data Symposium*, Purdue University, West Lafayette, Indiana, pp. 326-335, 1980

Markham B. L. & Barker J. L., Landsat MSS and TM post-calibration dynamic ranges, Exoatmospheric Reflectances and At-Satellite Temperatures*, EOSAT Landsat technical notes, 1*, pp. 3-8, 1986

Masek J.G., Honzak M.M Goward S.N, Liu P., Pak E., Landsat-7 ETM+ as an observatory for land cover initial radiometric and geometric comparisons with Landsat-5 Thematic Mapper*, Remote Sensing of Environment, 78*, pp. 118-130, 2001

Mattsson J.O., Rapp A., The recent droughts in western Ethiopia and Sudan in a climatic context, *Ambio, 20*, pp. 172-175, 1991

Mayaux P., Janodet E., Richards T., A vegetation map of central Africa derived from satellite imagery, *Journal of Biogeography, 25*, pp. 353-366, 1999

Middleton N.J., Thomas D.S.G., World atlas of desertification, Arnold, London, 1997

Nicholson S.E., Farrar T.J., The influence of soil type on the relationship between NDVI, rainfall and soil moisture in semi-arid Botswana, *Remote Sensing Environment, 50*, pp. 121-133, 1994

Nicholson S.E., Tucker C.J., Ba M.B., Desertification, drought and surface vegetation: An example from the west African Sahel, *Bulletin of the American Meteorological Society, 79*, pp. 815-829, 1998

Olsson L., On the causes of famine, drought, desertification and market failure in the Sudan, *Ambio, 22,* pp. 395-403, 1993

Prince S.D., A model of regional primary production for use with coarse resolution satellite data, *International Journal of Remote Sensing, 12*, pp. 1313-1330, 1991

Prince S.D, Goward S.N., Evaluation of the NOAA/NASA Pathfinder AVHRR land dataset for global primary production modelling, *International Journal of Remote Sensing,* 17, pp. 121-136, 1996

Prince S.D., Brown De Colstoun E., Kravitz L.L., Evidence from rain-use efficiencies does not indicate extensive sahelian desertification, *Global Change Biology, 4,* pp. 359-374, 1998

Rasmussen K., Fog D., Madsen, J.E., Desertification in reverse? Observations from northern Burkina Faso, *Global Environmental Change, 11*, pp. 271-282, 2001

Rayanaut C., Societies and Nature in the Sahel: Ecological diversity and social dynamics, *Global Environmental Change, 11*, pp. 9-18, 2001

Roy, D.P., The impact of misregistration upon composited wide field of view satellite data and implications for change detection, *IEEE Transactions on Geoscience and Remote Sensing, 38*, pp. 2017-2032, 2000

Runnström M.C., Is northern China winning the battle against desertification? Satellite remote sensing as a tool to study biomass trends on the Ordos plateau in semi-arid China, *Ambio, 29*, pp. 468-476, 2000

Runnström M.C., Rangeland development of the Mu Us sandy land in semi-arid china: an analysis using Landsat and NOAA remote sensing data, *Wiley InterScience,* 14, pp. 189-202, 2003

Seaquist, J., Mapping primary production for the West African Sahel with satellite data., *Meddelanden från Lunds Universitets Geografiska Instutitioner,* Avhandlingar 140, 2001

Slayback D.A., Pinzon J.E., Los S.O., Tucker C.J., Northern hemisphere photosynthetic trends 1982-99, *Global Change Biology, 9,* pp. 1-15, 2003

Sohl T., Change analysis in the United Arab Emirates, and investigation of techniques, *Photgrammetric Engineering and Remote Sensing, 65,* pp. 475-484, 1999

Steven M.D., Malthus T.J., Baret F., Xu H., Chopping M.J., Intercalibration of vegetation indices from different sensor systems, *Remote Sensing of Environment, 88,* 2003

Thiam A.K., The causes and spatial pattern of land degradation risk in southern Mauritania using multitemporal AVHRR-NDVI imagery and field data, *Land Degradation and Development, 14,* pp. 133-142, 2003

Tucker C.J., Dregne H.E., Newcomb W.W., Expansion and contraction of the Sahara desert from 1980 to 1990, *Science,* 253, pp. 299-301, 1991

Uchida S., Discrimination of agricultural land-use using multi-temporal NDVI data, Paper presented at the 22nd Asian Conference on Remote Sensing*,* National University of Singapore, 2001

United Nations (UN), Agenda 21: The United Nations plan of action from Rio, United Nations, New York, 1992

United States Department of Agriculture (USDA), National Resources Conservation Service (NRCS), Soil Taxonomy: A basic system of soil classification for making and interpreting soil surveys, 2nd Edition, Washington DC, 1999

Van Asten P.J.A., Van't Zelfde J.A., Van Der Zee S.E.A.T.M, Hammecker C., The effect of irrigated rice cropping on the alkalinity of two alkaline rice soils in the Sahel, *Geoderma, 119*, pp. 233-247, 2004

Vogelmann J.E., Helder D., Morfitt R., Choate M.J., Mercant J.W., Bulley H., Effects of Landsat 5 Thematic Mapper and Landsat 7 Enhanced Thematic Mapper Plus radiometric and geometric calibrations and corrections on landscape characterization, *Remote Sensing of Environment, 78,* pp. 55-70, 2001

Wezel A., Haigis J., Fallow Cultivation System and Farmers Resource Management in Niger, West Africa, *Land Degradation &Development,* 13*,* pp. 221-231, 2002

Wezel A., Schlecht E., Inter-annual variation of species composition of fallow vegetation in semi-arid Niger, *Journal of Arid Environments, 56,* pp. 265-282, 2004

Williams, M.A.J., Balling R.R., desertification and climatic change, 2nd edition, Edward Arnold, London, 1995

Yuan D., Elvidge C.D., Comparison of relative radiometric normalization techniques, *Journal of Photogrammetry and Remote Sensing, 51*, pp. 117-126, 1996

Internet Resources

Africover
http://www.africover.org/, 2004-03-03

Earth Observing System (EOS) Data Gateway
http://edcimswww.cr.usgs.gov/pub/imswelcome/, 2004-02-24

Earth Satellite Corporation (EarthSat)
http://www.earthsat.com/home.html, 2004-02-10

Global Historical Climatology Network (GHCN)
http://cdiac.esd.ornl.gov/ghcn/ghcn.html, 2004-03-03

Global Land Cover Facility (GLCF)
http://glcf.umiacs.umd.edu/index.shtml, 2004-02-10

USGS (US Geological survey) - NASA Distributed Active Archive Center (DAAC)
http://edcdaac.usgs.gov/glcc/af_int.asp, 2004-03-03

Appendix

Table A.1. Land cover change matrix for study site 1A located in the Sudan.

	To 1999				
Cover categories	Grassland	Open shrubs and herbaceous vegetation	Closed shrubland	Open trees and herbaceous vegetation	
From 1984					
Grassland	65.6	26.1	2.6	5.8	100.0
Open shrubs and herbaceous vegetation	2.2	70.3	27.5	0.0	100.0
Closed shrubland	0.1	28.6	71.2	0.0	100.0
Open trees and herbaceous vegetation	4.7	0.2	0.0	95.1	100.0

Table A.2. Land cover change matrix for study site 1B located in the Sudan.

	To 1999					
Cover categories	Grassland	Open shrubs and herbaceous vegetation	Closed shrubland	Open trees and herbaceous vegetation	Barren or sparsely vegetated (burnt areas)	
From 1984						
Grassland	26.6	43.4	29.6	0.4	0.0	100.0
Open shrubs and herbaceous vegetation	8.1	47.8	34.8	9.3	0.0	100.0
Closed shrubland	1.9	18.7	64.7	14.7	0.0	100.0
Open trees and herbaceous vegetation	0.0	25.5	63.9	10.6	0.0	100.0
Barren or sparsely vegetated (Burnt areas)	2.5	57.1	33.3	7.0	0.0	100.0

Table A.3. Land cover change matrix for study site 1C located in the Sudan.

						To 1999	
Cover categories	Grassland	Open shrubs and herbaceous vegetation	Closed shrubland	Open trees and herbaceous vegetation	Closed woodland	Rainfed cropland	
From 1984							
Grassland	20.0	13.0	2.9	29.7	1.9	32.5	100.0
Open shrubs and herbaceous vegetation	19.8	23.7	5.6	46.9	3.9	0.1	100.0
Closed shrubland	0.0	40.9	21.9	37.1	0.0	0.0	100.0
Open trees and herbaceous vegetation	3.1	1.6	0.0	82.9	10.2	2.2	100.0
Closed woodland	0.0	0.0	0.0	62.1	37.9	0.0	100.0
Rainfed cropland	15.3	15.2	12.7	9.8	0.0	47.0	100.0

Table A.4. Land cover land use change matrix for study site 2A located in the C.A.R.

					To 1999	
Cover categories	Open shrubs and herbaceous vegetation	Open trees and herbaceous vegetation	Closed woodland	Irrigated cropland	Water	
From 1984						
Open shrubs and herbaceous vegetation	74.6	17.6	0.2	7.6	0.0	100.0
Open trees and herbaceous vegetation	1.6	89.8	0.2	8.4	0.0	100.0
Closed woodland	0.6	6.1	81.7	11.6	0.0	100.0
Irrigated cropland	1.8	14.9	1.8	81.4	0.0	100.0
Water	0.0	0.0	0.0	0.0	100.0	100.0

Table A.5. Land cover change matrix for study site 3A located in Mauritania.

			To 1999		
Cover categories	Barren or sparsely vegetated	Open shrubs and herbaceous vegetation	Closed shrubland	Water	
From 1984					
Barren or sparsely vegetated	57.5	32.6	9.8	0.1	100.0
Open shrubs and herbaceous vegetation	5.7	58.9	34.7	0.7	100.0
Closed shrubland	11.5	19.6	64.2	4.7	100.0
Water	0.0	0.0	0.0	0.0	0.0

Previous reports

Lunds Universitets Naturgeografiska institution. Seminarieuppsatser. Uppsatserna finns tillgängliga på Naturgeografiska institutionens bibliotek, Sölvegatan 12, 223 62 LUND.

The reports are available at the Geo-Library, Department of Physical Geography, University of Lund, Sölvegatan 12, S-223 62 Lund, Sweden.

1. Pilesjö, P. (1985): Metoder för morfometrisk analys av kustområden.
2. Ahlström, K. & Bergman, A. (1986): Kartering av erosionskänsliga områden i Ringsjöbygden.
3. Huseid, A. (1986): Stormfällning och dess orsakssamband, Söderåsen, Skåne.
4. Sandstedt, P. & Wällstedt, B. (1986): Krankesjön under ytan - en naturgeografisk beskrivning.
5. Johansson, K. (1986): En lokalklimatisk temperaturstudie på Kungsmarken, öster om Lund.
6. Estgren, C. (1987): Isälvsstråket Djurfälla-Flädermo, norr om Motala.
7. Lindgren, E. & Runnström, M. (1987): En objektiv metod för att bestämma läplanteringars läverkan.
8. Hansson, R. (1987): Studie av frekvensstyrd filtringsmetod för att segmentera satellitbilder, med försök på Landsat TM-data över ett skogsområde i S. Norrland.
9. Matthiesen, N. & Snäll, M. (1988): Temperatur och himmelsexponering i gator: Resultat av mätningar i Malmö.
10A. Nilsson, S. (1988): Veberöd. En beskrivning av samhällets och bygdens utbyggnad och utveckling från början av 1800-talet till vår tid.
10B. Nilson, G., 1988: Isförhållande i södra Öresund.
11. Tunving, E. (1989): Översvämning i Murciaprovinsen, sydöstra Spanien, november 1987.
12. Glave, S. (1989): Termiska studier i Malmö med värmebilder och konventionell mätutrustning.
13. Mjölbo, Y. (1989): Landskapsförändringen - hur skall den övervakas?
14. Finnander, M-L. (1989): Vädrets betydelse för snöavsmältningen i Tarfaladalen.
15. Ardö, J. (1989): Samband mellan Landsat TM-data och skogliga beståndsdata på avdelningsnivå.
16. Mikaelsson, E. (1989): Byskeälvens dalgång inom Västerbottens län. Geomorfologisk karta, beskrivning och naturvärdesbedömning.
17. Nhilen, C. (1990): Bilavgaser i gatumiljö och deras beroende av vädret. Litteraturstudier och mätning med DOAS vid motortrafikled i Umeå.
18. Brasjö, C. (1990): Geometrisk korrektion av NOAA AVHRR-data.
19. Erlandsson, R. (1991): Vägbanetemperaturer i Lund.
20. Arheimer, B. (1991): Näringsläckage från åkermark inom Brååns dräneringsområde. Lokalisering och åtgärdsförslag.
21. Andersson, G. (1991): En studie av transversalmoräner i västra Småland.
22A. Skillius, Å., (1991): Water havesting in Bakul, Senegal.
22B. Persson, P. (1991): Satellitdata för övervakning av höstsådda rapsfält i Skåne.
23. Michelson, D. (1991): Land Use Mapping of theThat Luang - Salakham Wetland, Lao PDR, Using Landsat TM-Data.
24. Malmberg, U. (1991): En jämförelse mellan SPOT- och Landsatdata för vegetations-klassning i Småland.

25. Mossberg, M. & Pettersson, G. (1991): A Study of Infiltration Capacity in a Semiarid Environment, Mberengwa District, Zimbabwe.
26. Theander, T. (1992): Avfallsupplag i Malmöhus län. Dränering och miljöpåverkan.
27. Osaengius, S. (1992): Stranderosion vid Löderups strandbad.
28. Olsson, K. (1992): Sea Ice Dynamics in Time and Space. Based on upward looking sonar, satellite images and a time series of digital ice charts.
29. Larsson, K. (1993): Gully Erosion from Road Drainage in the Kenyan Highlands. A Study of Aerial Photo Interpreted Factors.
30. Richardson, C. (1993): Nischbildningsprocesser - en fältstudie vid Passglaciären, Kebnekaise.
31. Martinsson, L. (1994): Detection of Forest Change in Sumava Mountains, Czech Republic Using Remotely Sensed Data.
32. Klintenberg, P. (1995): The Vegetation Distribution in the Kärkevagge Valley.
33. Hese, S. (1995): Forest Damage Assessment in the Black Triangle area using Landsat TM, MSS and Forest Inventory data.
34. Josefsson, T. och Mårtensson, I. (1995). A vegetation map and a Digital Elevation Model over the Kapp Linné area, Svalbard -with analyses of the vertical and horizontal distribution of the vegetation.
35. Brogaard, S och Falkenström, H. (1995). Assessing salinization, sand encroachment and expanding urban areas in the Nile Valley using Landsat MSS data.
36. Krantz, M. (1996): GIS som hjälpmedel vid växtskyddsrådgivning.
37. Lindegård, P. (1996). Vinterklimat och vårbakslag. Lufttemperatur och kådflödessjuka hos gran i södra Sverige.
38. Bremborg, P. (1996). Desertification mapping of Horqin Sandy Land, Inner Mongolia, by means of remote sensing.
39. Hellberg, J. (1996). Förändringsstudie av jordbrukslandskapet på Söderslätt 1938-1985.
40. Achberger, C. (1996): Quality and representability of mobile measurements for local climatological research.
41. Olsson, M. (1996): Extrema lufttryck i Europa och Skandinavien 1881-1995.
42. Sundberg, D. (1997): En GIS-tillämpad studie av vattenerosion i sydsvensk jordbruksmark.
43. Liljeberg, M. (1997): Klassning och statistisk separabilitetsanalys av marktäckningsklasser i Halland, analys av multivariata data Landsat TM och ERS-1 SAR.
44. Roos, E. (1997): Temperature Variations and Landscape Heterogeneity in two Swedish Agricultural Areas. An application of mobile measurements.
45. Arvidsson, P. (1997): Regional fördelning av skogsskador i förhållande till mängd SO_2 under vegetationsperioden i norra Tjeckien.
46. Akselsson, C. (1997): Kritisk belastning av aciditet för skogsmark i norra Tjeckien.
47. Carlsson, G. (1997): Turbulens och supraglacial meandring.
48. Jönsson, C. (1998): Multitemporala vegetationsstudier i nordöstra Kenya med AVHRR NDVI
49. Kolmert, S. (1998): Evaluation of a conceptual semi-distributed hydrological model – A case study of Hörbyån.
50. Persson, A. (1998): Kartering av markanvändning med meteorologisk satellitdata för förbättring av en atmosfärisk spridningsmodell.
51. Andersson, U. och Nilsson, D. (1998): Distributed hydrological modelling in a

GIS perspective – an evaluation of the MIKE SHE model.
52. Andersson, K. och Carlstedt, J. (1998): Different GIS and remote sensing techniques for detection of changes in vegetation cover - A study in the Nam Ngum and Nam Lik catchment areas in the Lao PDR.
53. Andersson, J., (1999): Användning av global satllitdata för uppskattning av spannmålsproduktion i västafrikanska Sahel.
54. Flodmark, A.E., (1999): Urban Geographic Information Systems, The City of Berkeley Pilot GIS
55A. Lyborg, Jessic & Thurfell, Lilian (1999): Forest damage, water flow and digital elevation models: a case study of the Krkonose National Park, Czech Republic.
55B. Tagesson, I., och Wramneby, A., (1999): Kväveläckage inom Tolångaåns dräneringsområde – modellering och åtgärdssimulering.
56. Almkvist, E., (1999): Högfrekventa tryckvariationer under de senaste århundradena.
57. Alstorp, P., och Johansson, T., (1999): Översiktlig buller- och luftföroreningsinventering i Burlövs Kommun år 1994 med hjälp av geografiska informationssystem – möjligheter och begränsningar.
58. Mattsson, F., (1999): Analys av molnklotter med IRST-data inom det termala infraröda våglängdsområdet
59. Hallgren, L., och Johansson, A., (1999): Analysing land cover changes in the Caprivi Strip, Namibia, using Landsat TM and Spot XS imagery.
60. Granhäll, T., (1999): Aerosolers dygnsvariationer och långväga transporter.
61. Kjellander, C., (1999): Variations in the energy budget above growing wheat and barley, Ilstorp 1998 - a gradient-profile approach
62. Moskvitina, M., (1999): GIS as a Tool for Environmental Impact Assessment - A case study of EIA implementation for the road building project in Strömstad, Sweden
63. Eriksson, H., (1999): Undersökning av sambandet mellan strålningstemperatur och NDVI i Sahel.
64. Elmqvist, B., Lundström, J., (2000): The utility of NOAA AVHRR data for vegetation studies in semi-arid regions.
65. Wickberg, J., (2000): GIS och statistik vid dräneringsområdesvis kväveläckagebeskrivning i Halland.
66. Johansson, M., (2000): Climate conditions required for re-glaciation of cirques in Rassepautasjtjåkka massif, northern Sweden.
67. Asserup, P., Eklöf, M., (2000): Estimation of the soil moisture distribution in the Tamne River Basin, Upper East Region, Ghana.
68. Thern, J., (2000): Markvattenhalt och temperatur i sandig jordbruksmark vid Ilstorp, centrala Skåne: en mätnings- och modelleringsstudie.
69. Andersson, C., Lagerström, M., (2000): Nitrogen leakage from different land use types - a comparison between the watersheds of Graisupis and Vardas, Lithuania.
70. Svensson, M., (2000): Miljökonsekvensbeskrivning med stöd av Geografiska Informationssystem (GIS) – Bullerstudie kring Malmö-Sturup Flygplats.
71. Hyltén, H.A., Uggla, E., (2000): Rule.Based Land Cover Classification and Erosion Risk Assessment of the Krkonoše National Park, Czech Republic.
72. Cronquist, L., Elg, S., (2000): The usefulness of coarse resolution satellite sensor data for identification of biomes in Kenya.
73. Rasmusson, A-K., (2000): En studie av landskapsindex för kvantifiering av rumsliga landskapsmönster.

74. Olofsson, P., Stenström, R., (2000): Estimation of leaf area index in southern Sweden with optimal modelling and Landsat 7 ETM+Scene.
75. Uggla, H., (2000): En analys av nattliga koldioxidflöden i en boreal barrskog avseende spatial och temporal variation.
76. Andersson, E., Andersson, S., (2000): Modellering och uppmätta kväveflöden i energiskog som bevattnas med avloppsvatten.
77. Dawidson, E., Nilsson, C., (2000): Soil Organic Carbon in Upper East Region, Ghana - Measurements and Modelling.
78. Bengtsson, M., (2000): Vattensänkningar - en analys av orsaker och effekter.
79. Ullman, M., (2001): El Niño Southern Oscillation och dess atmosfäriska fjärrpåverkan.
80. Andersson, A., (2001): The wind climate of northwestern Europe in SWECLIM regional climate scenarios.
81. Lalloo, D., (2001): Geografiska informationssystem för studier av polyaromatiska kolväten (PAH) – Undersökning av djupvariation i BO01-området, Västra hamnen, Malmö, samt utveckling av en matematisk formel för beräkning av PAH-koncentrationer från ett kontinuerligt utsläpp.
82. Almqvist, J., Fergéus, J., (2001): GIS-implementation in Sri Lanka.
Part 1: GIS-applications in Hambantota district Sri Lanka : a case study.
Part 2: GIS in socio-economic planning : a case study.
83. Berntsson, A., (2001): Modellering av reflektans från ett sockerbetsbestånd med hjälp av en strålningsmodell.
84. Umegård, J., (2001): Arctic aerosol and long-range transport.
85. Rosenberg, R., (2002): Tetratermmodellering och regressionsanalyser mellan topografi, tetraterm och tillväxt hos sitkagran och lärk – en studie i norra Island.
86. Håkansson, J., Kjörling, A., (2002): Uppskattning av mängden kol i trädform – en metodstudie.
87. Arvidsson, H., (2002): Coastal parallel sediment transport on the SE Australian inner shelf – A study of barrier morphodynamics.
88. Bemark, M., (2002): Köphultssjöns tillstånd och omgivningens påverkan.
89. Dahlberg, I., (2002): Rödlistade kärlväxter i Göteborgs innerstad – temporal och rumslig analys av rödlistade kärlväxter i Göteborgs artdataarkiv, ADA.
90. Poussart, J-N., (2002): Verification of Soil Carbon Sequestration - Uncertainties of Assessment Methods.
91. Jakubaschk, C., (2002): Acacia senegal, Soil Organic Carbon and Nitrogen Contents: A Study in North Kordofan, Sudan.
92. Lindqvist, S., (2002): Skattning av kväve i gran med hjälp av fjärranalys.
93. Göthe, A., (2002): Översvämningskartering av Vombs ängar.
94. Lööv, A., (2002): Igenväxning av Köphultasjö – bakomliggande orsaker och processer.
95. Axelsson, H., (2003): Sårbarhetskartering av bekämpningsmedels läckage till grundvattnet – Tillämpat på vattenskyddsområdet Ignaberga-Hässleholm.
96. Hedberg, M., Jönsson, L., (2003): Geografiska Informationssystem på Internet – En webbaserad GIS-applikation med kalknings- och försurningsinformation för Kronobergs län.
97. Svensson, J., (2003): Wind Throw Damages on Forests – Frequency and Associated Pressure Patterns 1961-1990 and in a Future Climate Scenario.
98. Stroh, E., (2003): Analys av fiskrättsförhållandena i Stockholms skärgård i

relation till känsliga områden samt fysisk störning.

99. Bäckstrand, K., (2004): The dynamics of non-methane hydrocarbons and other trace gas fluxes on a subarctic mire in northern Sweden.
100. Hahn, K., (2004): Termohalin cirkulation i Nordatlanten.
101. Lina Möllerström (2004): Modelling soil temperature & soil water availability in semi-arid Sudan: validation and testing.
102. Setterby, Y., (2004): Igenväxande hagmarkers förekomst och tillstånd i Västra Götaland.
103. Edlundh, L., (2004): Utveckling av en metodik för att med hjälp av lagerföljdsdata och geografiska informationssystem (GIS) modellera och rekonstruera våtmarker i Skåne.
104. Schubert, P., (2004): Cultivation potential in Hambantota district, Sri Lanka
105. Brage, T., (2004): Kvalitetskontroll av servicedatabasen Sisyla
106. Sjöström., M., (2004): Investigating vegetation changes in the African Sahel 1982-2002: a comparative analysis using Landsat, MODIS and AVHRR remote sensing data
107. Danilovic, A., Stenqvist, M., (2004): Naturlig föryngring av skog
108. Materia, S., (2004): Forests acting as a carbon source: analysis of two possible causes for Norunda forest site
109. Hinderson, T., (2004): Analysing environmental change in semi-arid areas in Kordofan, Sudan
110. Andersson, J., (2004): Skånska småvatten nu och då - jämförelse mellan 1940, 1980 och 2000-talet